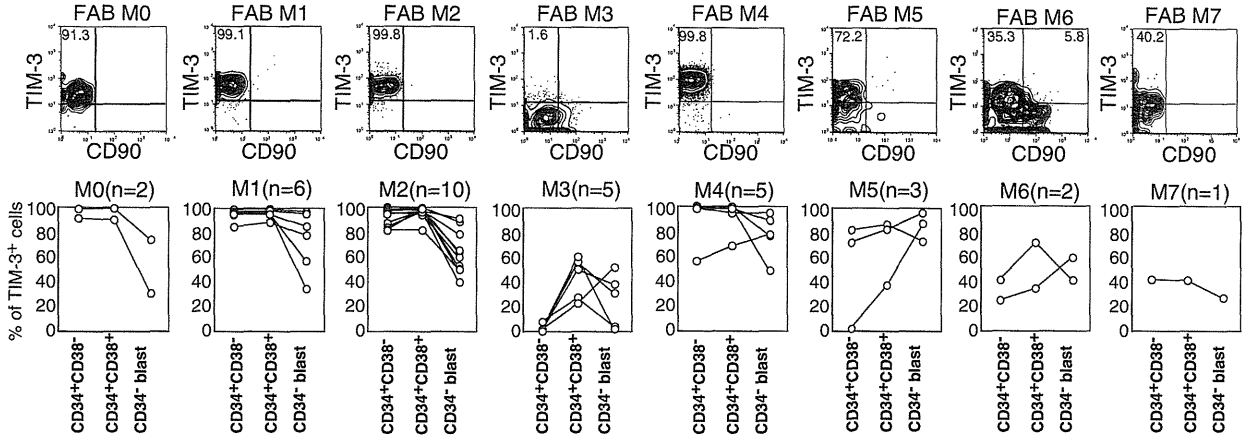

Figure 2. The Expression of TIM-3 in Stem and Progenitor Populations of AML of Each FAB Type
Expression of TIM-3 in each FAB type of AML. The representative expression pattern of TIM-3 in the $CD34^+CD38^-$ LSC fraction (top) and distribution of TIM-3 in $CD34^+CD38^-$ LSCs, $CD34^+CD38^+$ leukemic progenitors, and $CD34^-$ leukemic blasts (bottom) are shown.

expressed TIM-3. TIM-3 was, however, not expressed in the $CD34^+CD38^-$ population in all five M3 cases tested. In general, TIM-3 was expressed in both $CD34^+CD38^-$ LSCs and $CD34^+CD38^+$ leukemic progenitor fractions, but its expression tended to decline at the $CD34^-$ leukemic blast stage (**Figure 2**, bottom).

The TIM-3-Expressing of AML Fraction Contains the Vast Majority of Functional LSCs in a Xenograft Model

Recent studies have suggested that at least in some AML cases, LSCs that are capable of initiating human AML in xenograft models reside not only within the $CD34^+CD38^-$ fraction but also outside of this population including $CD34^+CD38^+$ (**Taussig et al., 2008**) or $CD34^-$ (**Martelli et al., 2010; Taussig et al., 2010**) AML cells. To evaluate whether functional AML LSCs express TIM-3, 10^6 cells of human TIM-3^+ and TIM-3^- AML populations were transplanted into sublethally irradiated immunodeficient mice. We used NOD.Cg-*Rag1*^{tm1Mom} *Il2rg*^{tm1Wjl}/SzJ (NRG) mice for the xenogeneic transplantation experiments, by which higher chimerism of human hematopoietic cells was observed in xenotransplantation assays (**Pearson et al., 2008**). Recipients transplanted with TIM-3^+ and TIM-3^- AML cells were sacrificed 8–10 weeks after transplantation. As shown in **Figure 3**, human $CD45^+CD33^+$ AML cells were

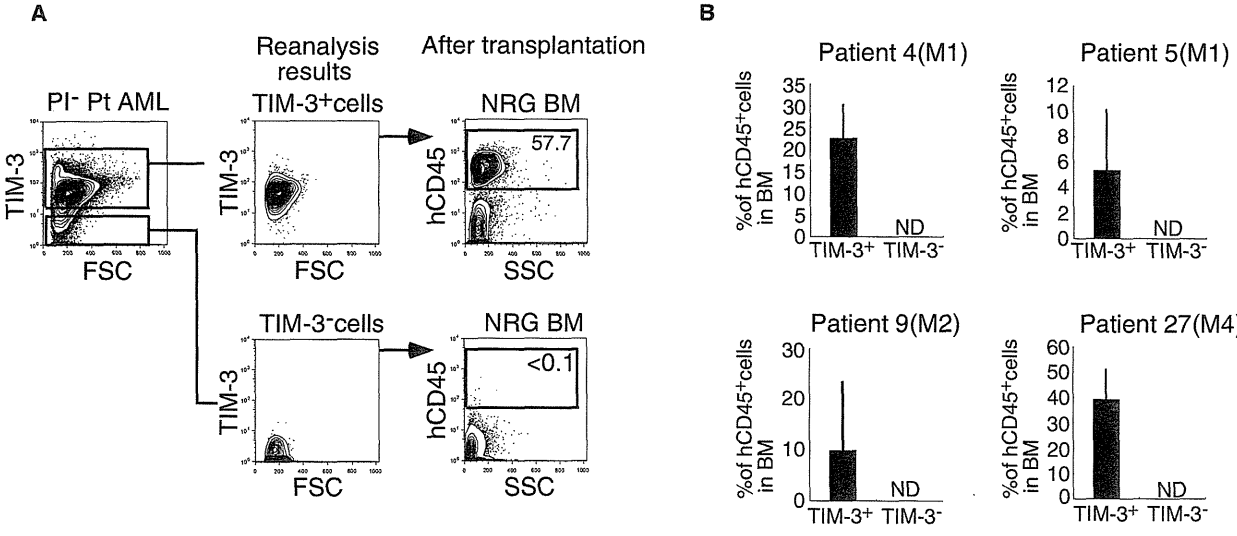

Figure 3. The TIM-3^+ AML Population Contains the Vast Majority of Functional LSC Activity
(A) A representative analysis of xenotransplantation of purified TIM-3^+ or TIM-3^- AML cells from patient 27 into NRG mice. Only TIM-3^+ cells reconstitute $hCD45^+$ AML cells after transplantation.
(B) Summarized data of four independent experiments. Only TIM-3^+ (not TIM-3^-) AML cells reconstituted human AML cells in xenotransplantation experiments in all experiments, suggesting that most functional LSCs reside in the TIM-3^+ AML fraction.

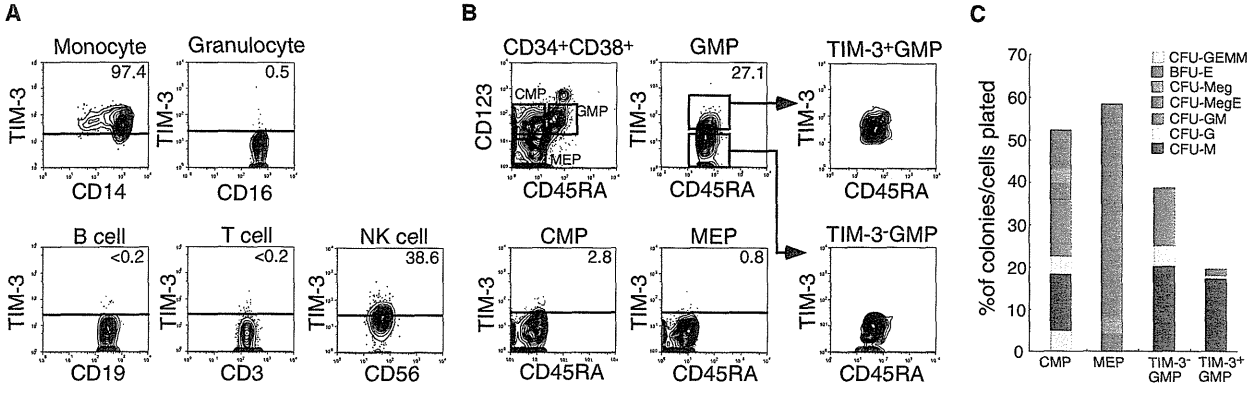

Figure 4. TIM-3 Is Expressed in Monocytes and Their Progenitors in Normal Hematopoiesis

(A) TIM-3 expression in normal mature blood cells.

(B) TIM-3 expression in normal hematopoietic progenitors. A fraction of GMPs but not other myeloid progenitors express TIM-3.

(C) Results of clonogenic assays of myelo-erythroid progenitors including single TIM-3$^+$ GMPs out of five independent experiments. The vast majority of TIM-3$^+$ GMPs gave rise to macrophage colonies (CFU-M).

reconstituted only in mice transplanted with TIM-3$^+$ AML cells, whereas TIM-3$^-$ AML cells failed to reconstitution in all four AML cases tested (**Figure 3B**). Thus, all 23 mice injected with TIM-3$^+$ AML cells reconstituted human AML, whereas 11 mice injected with TIM-3$^-$ AML never developed human AMLs after transplantation. These results strongly suggest that LSCs exclusively reside within the TIM-3$^+$ fraction in human AML at least in these patients.

TIM-3 Is Not Expressed in Normal Adult HSCs, and Its Expression Begins after Cells Are Committed to the Monocyte Lineage

Murine TIM-3 is expressed in a fraction of Th1 cells, monocytes, dendritic cells, and mast cells (**Anderson et al., 2007; Monney et al., 2002; Nakae et al., 2007**). The expression of human TIM-3 protein in normal steady-state human hematopoiesis is shown in **Figures 4**A. In periphery, TIM-3 was expressed in monocytes and a fraction of NK cells, but not in granulocytes, T cells, or B cells (**Figure 4**A). In the bone marrow, TIM-3 was not expressed in normal HSCs (**Figure 1**) or the vast majority of the CD34$^+$CD38$^+$ progenitor population. Within the CD34$^+$CD38$^+$ fraction, TIM-3 was expressed only in a fraction of GMPs at a low level, but not in common myeloid progenitors (CMPs), megakaryocyte/erythrocyte progenitors (MEPs) (**Figure 4**B), or common lymphoid progenitors (CLPs) (not shown). In clonogenic colony-forming unit (CFU) assays, the vast majority of purified TIM-3$^+$ GMPs gave rise to CFU-M, whereas colonies derived from TIM-3$^-$ GMP contained CFU-GM as well as CFU-G and CFU-M (**Figure 4**C). These data strongly suggest that TIM-3 upregulation mainly occurs in concert with the monocyte lineage commitment at the GMP stage in normal hematopoiesis.

Anti-Human TIM-3 Antibodies Did Not Impair Development of Normal Hematopoiesis

To selectively eliminate TIM-3-expressing AML LSCs in vivo, we developed a monoclonal antibody against TIM-3 that has an efficient interaction with cellular Fc receptors on innate immune effector cells. It has become clear that the ADCC activity is one of the most important factors to eliminate target cells in antibody therapies (**Nimmerjahn and Ravetch, 2007**). A TIM-3 monoclonal antibody (IgG2b) was obtained by immunizing Balb/c mice with L929 cells stably expressing human TIM-3 and soluble TIM-3 protein. The variable portion of the VH regions of the cloned hybridoma that recognize TIM-3 were then grafted onto IgG2a Fc regions, because IgG2a subclass is most efficient to induce ADCC activity in mice (**Nimmerjahn and Ravetch, 2005; Uchida et al., 2004**). The established clone, ATIK2a, possessed CDC activities in EoL-1 and L929 cells transfected with TIM-3 (**Figure 5**A), as well as Kasumi-3, an AML cell line that spontaneously expresses TIM-3 (not shown). Importantly, ATIK2a displayed strong ADCC activity against TIM-3-expressing EoL-1 and L929 cells in vitro (**Figure 5**B).

We first tested the effect of ATIK2a treatment on reconstitution of normal HSCs in a xenograft model. The major effectors in ADCC reaction are NK cells. Because NRG mice do not have NK cells because of γc mutation (**Pearson et al., 2008**), we used NOD-SCID mice for this experiment to potentiate ADCC activity of ATIK2a antibodies. NOD-SCID mice were sublethally irradiated and were transplanted with 10^5 CD34$^+$ adult human bone marrow cells. 15 μg of ATIK2a was intraperitoneally injected to mice 12 hr after transplantation, which was followed by further injections of 15 μg of ATIK2a once a week until mice were sacrificed at 12 weeks after transplantation. Injection of ATIK2a did not affect reconstitution of normal hematopoiesis: The percentage of human cells were equal (~1%), and human B and myeloid cells were normally reconstituted irrespective of ATIK2a treatment in three independent experiments (not shown). We also tested the effect of this ATIK2a treatment in NOD-SCID mice transplanted with 10^5 CD34$^+$ cord blood cells. Cord blood cells have potent reconstitution activity in NOD-SCID mice, and percentage of hCD45$^+$ human cells reached ~50% after transplantation (**Figure 5**C). Again, the chimerism of human cells was equal, and CD19$^+$ B cells and CD33$^+$ myeloid cells were reconstituted irrespective of ATIK2a treatment (**Figure 5**C, left). In mice injected with ATIK2a, however, human TIM-3$^+$ monocytes were removed (**Figure 5**C, right). These data suggest that

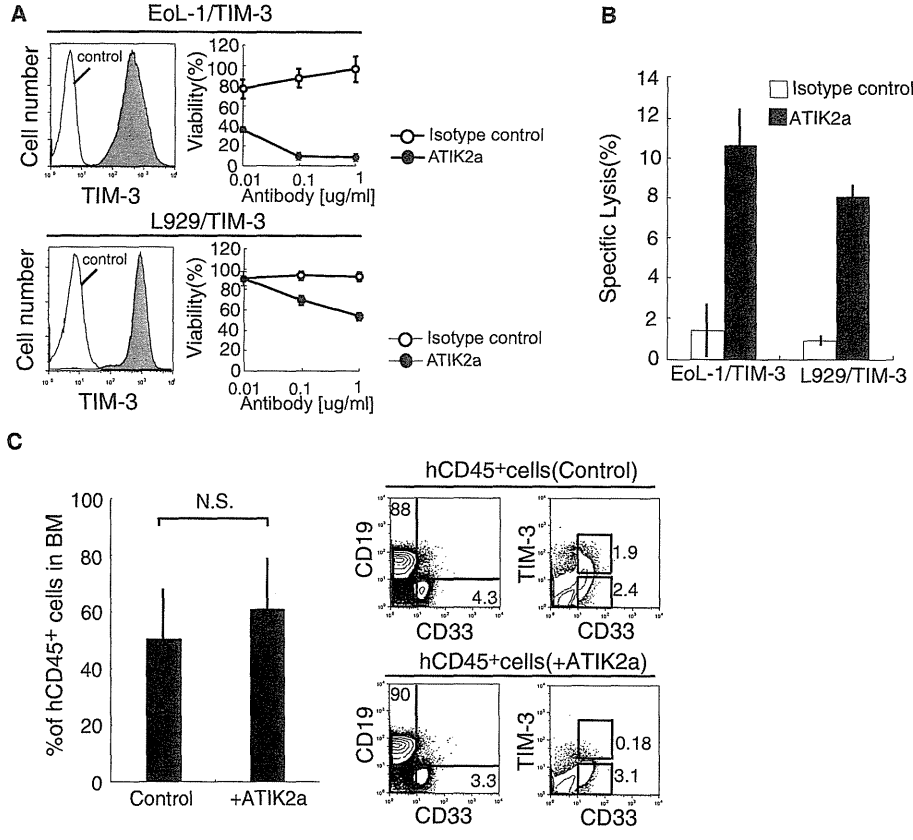

Figure 5. ATIK2a, a New Monoclonal Antibody against TIM-3, Has CDC and ADCC Activities and Does Not Harm Normal Hematopoietic Reconstitution

(A) CDC assays to evaluating the killing effect of ATIK2a antibodies on EoL-1 and L929 cell lines with enforced expression of human TIM-3.

(B) ADCC activities of ATIK2a on TIM-3-expressing EoL-1 and L929 cell lines.

(C) The effect of ATIK2a treatment on human hematopoietic reconstitution in NOD-SCID mice transplanted with 10^5 $CD34^+$ human cord blood cells. 15 μg of ATIK2a was intraperitoneally injected to mice 12 hr after transplantation, which was followed by further injections of 15 μg of ATIK2a once a week until mice were sacrificed at 12 weeks after transplantation. In this experiment, percentages of human cells in 10 each of mouse groups treated with control or ATIK2a antibodies were equivalent at 12 weeks after transplantation.

targeting TIM-3 does not affect development of normal hematopoiesis but remove TIM-3-expressing monocytes.

Anti-Human TIM-3 Antibodies Effectively Blocked Development of AML LSCs but Not that of Normal HSCs

We then tried to test the effect of ATIK2a in AML LSCs. We transplanted 10^6 bone marrow cells of AML patients (patients 6, 9, 15, 18, and 26) into NOD-SCID mice. The bone marrow of patients 6, 9, 15, and 26 were completely occupied with AML clones, and normal HSCs were not seen on FACS. Samples of each patient were transplanted into six mice, and three mice each were treated with 15 μg of ATIK2a or control IgG 12 hr after transplantation and with the same dose of antibodies once a week (**Figure 6**A). Mice were sacrificed 16 weeks after xenotransplantation. As shown in **Figure 6**B, the chimerism of AML cells were low in the NOD-SCID xenotransplant system. Nonetheless, ATIK2a injection significantly blocked AML reconstitution in these mice. In all of these patients, mice injected with control IgG showed reconstitution of $CD34^+TIM\text{-}3^+$ cells that contained primitive AML stem or progenitors as well as $CD33^+$ AML blasts (**Figure 6**B). In contrast, in mice treated with ATIK2a, the leukemic clone was barely detectable, and did not contain detectable numbers of $CD34^+$ cells (not shown), displaying significantly lower chimerisms as compared to control mice in all four independent experiments (**Figure 6**C).

The bone marrow of patient 18 possessed a small fraction of $CD34^+CD38^-CD90^+TIM\text{-}3^-$ cells that was phenotypically normal HSCs, in addition to the major fraction of $CD34^+CD38^-CD90^-TIM\text{-}3^+$ AML LSCs (**Figure 6**D). Interestingly, in mice transplanted with the bone marrow from this patient, ATIK2a injection induced reconstitution of normal myeloid and B cells, whereas control mice developed AML. These data strongly suggest that the ATIK2a treatment selectively inhibited development of human AML, presumably by targeting LSCs, instead allowing normal HSCs to reconstitute human hematopoiesis in vivo.

TIM-3 Targets Leukemic Stem Cells

In testing the inhibitory effect of ATIK2a on established human AML in a xenotransplant system, we used the NRG mice to increase engraftment efficiency of human AML cells. Eight

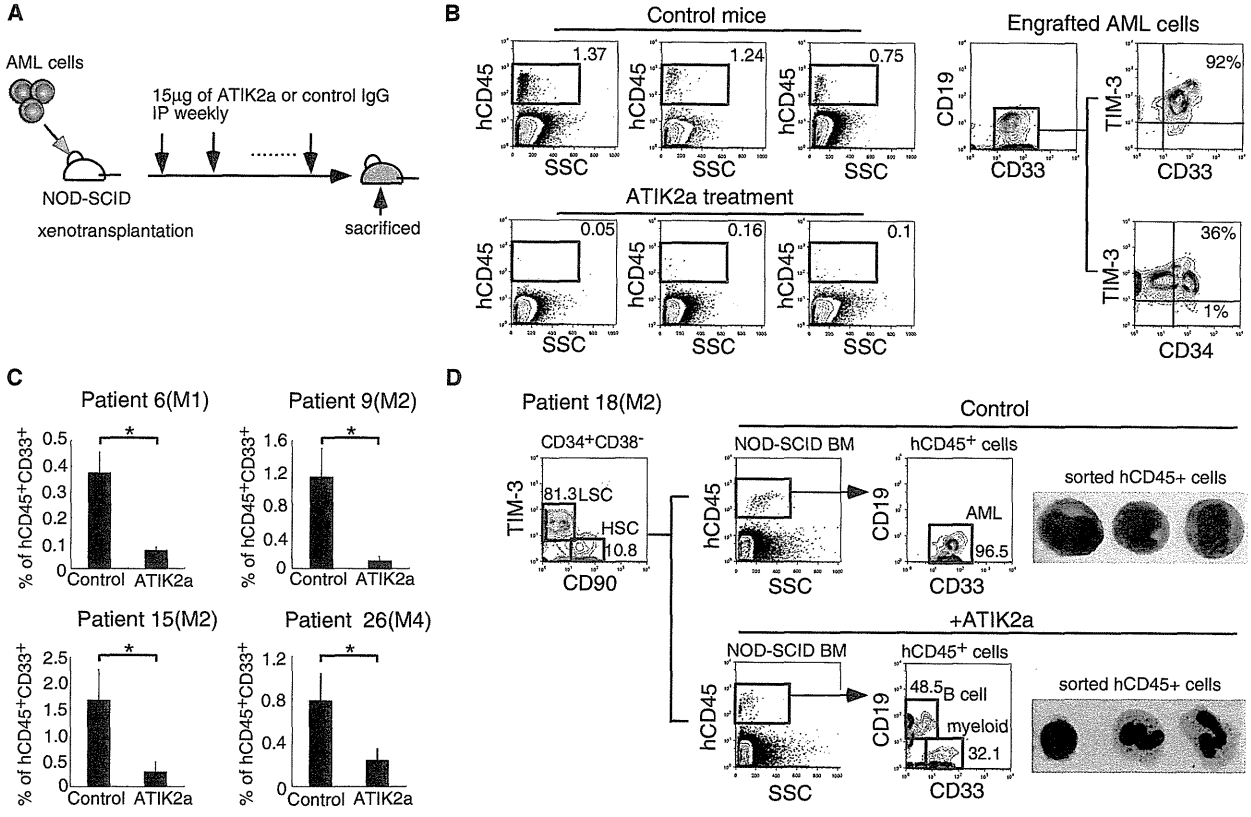

Figure 6. ATIK2a Antibodies Blocked AML Reconstitution in NOD-SCID Mice

(A) Schedule of ATIK2a administration in NOD-SCID experiment. ATIK2a treatment was started 12 hr after the transplantation.

(B) Analysis of mice transplanted with AML bone marrow cells at 16 weeks after transplantation. Three control mice (left top) showed reconstitution of human $CD45^+$ cells, and the majority of these cells were $TIM\text{-}3^+CD33^+$ AML cells that contained $CD34^+$ leukemic progenitor or stem cell populations (right). In contrast, mice treated with ATIK2a (left bottom) have only a small number of $hCD45^+$ cells. Representative data of patient 9 are shown.

(C) Summary of four independent experiments to test the effect of ATIK2a on reconstitution of AML bone marrow cells from patients 6, 9, 15, and 26. In all experiments, ATIK2a treatment significantly inhibited the AML reconstitution. Three mice per group were analyzed.

(D) Selective inhibition of AML reconstitution by ATIK2a in mice reconstituted with the bone marrow of patient 18, which contained both normal HSCs and AML LSCs (left). Injection of the bone marrow cells resulted in AML development in control mice (right top), whereas mice treated with ATIK2a developed normal hematopoiesis (right bottom).

weeks after injection of 10^6 AML cells, engraftment of human AML cells were confirmed by blood sampling. In NRG mice, ATIK2a cannot fully exert its ADCC effects because of a lack of NK cells. Therefore, we injected a high dose (80 μg) of ATIK2a to maximize its CDC effects on AML cells in vivo. These mice were treated with ATIK2a or control IgG, 3 times a week for 4 weeks (**Figure 7**A). In all four cases tested (patients 7, 14, 27, and 28), ATIK2a treatment significantly reduced human $CD45^+$ AML burden in vivo: ATIK2a strongly suppressed or eliminated the $TIM\text{-}3^+$ AML fraction (**Figure 7**B, left) that contains all functional LSCs in our hand (**Figure 3**B), as well as the $CD34^+CD38^-$ LSC fraction (**Figure 7**B, right, and **Figure 7**C), suggesting that reduction of leukemic burden by ATIK2a was achieved at least in part by killing LSCs.

In patients 7 and 27, in order to verify the anti-AML LSC effect of ATIK2a treatment, 10^6 human $CD45^+$ AML cells from the primary NRG recipients were further retransplanted into secondary NRG recipients. In patients 14 and 28, however, reduction of AML cells by ATIK2a in primary recipients was very severe, and we could not harvest sufficient numbers of AML cells to transplant into secondary recipients. We then evaluated the re-engraftment of AML cells in secondary recipients 8 weeks after transplantation. All seven mice transplanted with bone marrow cells from primary recipients treated with control IgG developed AML, whereas none of 10 mice transplanted with cells from ATIK2a-treated primary recipients developed AML. Representative data in patient 27 are shown in **Figure 7**C. These data again suggest that functional LSCs were effectively eliminated by ATIK2a treatment in primary recipients.

DISCUSSION

To selectively kill AML LSCs sparing normal HSCs, one of the most practical approaches is to target the AML LSC-specific surface or functionally indispensable molecules. To achieve specificity for LSCs, the target molecule should be expressed

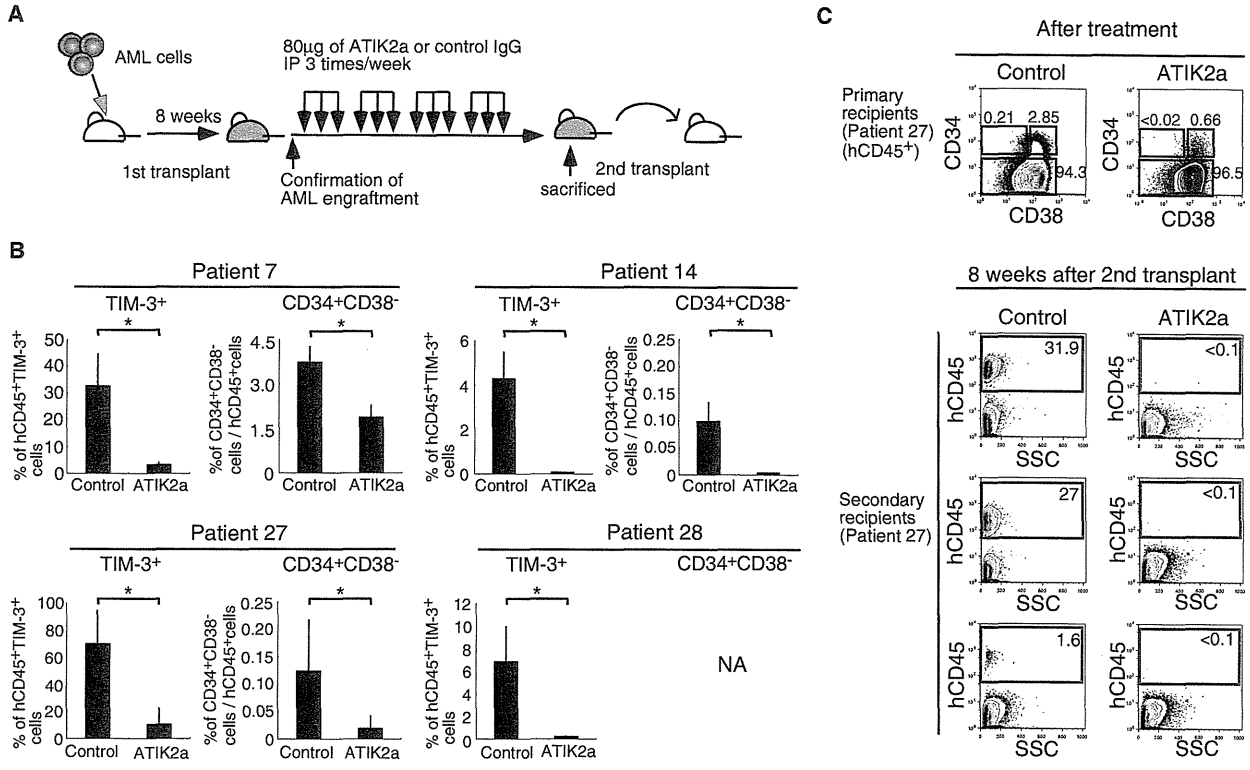

Figure 7. ATIK2a Antibodies Reduced the AML Burden at Least Targeting Functional LSCs

(A) Schedule of ATIK2a administration to test the effect on established human AML in NRG mouse experiments. ATIK2a treatment was started 8 weeks after transplantation.

(B) Summary of four independent experiments to assess the effect of ATIK2a on established human AML cells in vivo (patients 7, 14, 27, and 28). In all experiments, ATIK2a treatment significantly reduced hCD45$^+$ AML burden. Within the hCD45$^+$ population, the TIM-3$^+$ AML fraction that should contain AML LSCs (see **Figure 3**) was also reduced by this treatment. The percentages of CD34$^+$CD38$^-$ cells, in which LSCs were concentrated, were also reduced. Three to six mice in each group were analyzed.

(C) The phenotype of engrafted hCD45$^+$ cells in primary recipients (top). 10^6 hCD45$^+$ AML cells were then harvested from primary recipients treated with ATIK2a or control IgG, and then retransplanted into the secondary NRG recipients. ATIK2a efficiently blocked reconstitution of AML cells (bottom). Representative results of patient 27 are shown.

on LSCs at a high level but not on normal HSCs. In addition, when the molecule is expressed also in leukemic progenitors or blasts, it will help mass reduction of AML clones. It should not matter whether the molecule is expressed in normal mature blood cells or progenitor cells, because if normal HSCs are spared, they should be able to replenish all mature blood cells after treatment.

TIM-3 is expressed in the CD34$^+$CD38$^-$ AML LSC fraction as well as the majority of their downstream CD38$^+$ leukemic progenitors in most AML types except for M3. TIM-3$^+$ but not TIM-3$^-$ AML population engrafted and reconstituted human AML in NRG mice, suggesting that functional LSCs almost exclusively reside in TIM-3$^+$ cells. In contrast, normal HSCs do not express TIM-3. Thus, TIM-3 should be useful molecules to target AML LSCs without seriously affecting normal hematopoiesis. In steady-state human hematopoiesis, TIM-3 is not expressed in HSCs or myeloerythroid or lymphoid progenitor populations. TIM-3 expression begins at the GMP stage, in parallel with monocyte lineage commitment (**Figure 4**). Furthermore, in addition to TIM-3, the expression profiling data show that the CD34$^+$ CD38$^-$ LSC fraction expressed many monocyte lineage-related molecules such as CD86 and CSF1R at a high level (**Figure 1**). In this context, LSCs in most AML types, except for M3 that might be of granulocytic lineage leukemia, may activate some monocyte lineage-related programs.

ATIK2a, a TIM-3 antibody with ADCC and CDC activities, selectively blocked the human AML engraftment and/or development in NOD-SCID mice, whereas it did not disturb normal HSC engraftment. Furthermore, in NRG mice transplanted with human AML cells where percentage of engrafted human cells reached 5%–60% (**Figure 7**B), ATIK2a treatment reduced or eliminated CD34$^+$ CD38$^-$ and TIM-3$^+$ LSC-containing fractions within the bone marrow of primary recipients, resulting in failure of re-engraftment of primary recipients' bone marrow cells into secondary recipients (**Figure 7**C). Collectively, it is likely that ATIK2a eradicated functional AML LSCs in vivo, sparing normal HSCs.

To use surface markers for targeting AML LSCs, specificity as well as sensitivity should be critical. TIM-3 has an advantage against other candidate markers in several aspects: Detectable levels of TIM-3 protein is not expressed in normal HSCs or other

progenitors except for only a fraction of GMPs. Furthermore, TIM-3 is expressed in LSCs at a high level, and its expression was found in the vast majority of $CD34^+CD38^-$ cells of M0, M1, M2, and M4 AMLs in all cases tested. As shown in **Figure 1**, the mRNA expression level of CD25, CD32, CD44, and CD47 in LSCs was only 2- to 3-fold higher as compared to normal HSCs, and in some AML cases, LSCs did not express these molecules. CD33 and CD123 proteins were detectable in normal HSCs (**Figure 1**B) as well as most myeloid progenitors including CMPs and GMPs (**Taussig et al., 2005**). In fact, prolonged cytopenias have been observed in AML patients treated with gemtuzumab, a recombinant humanized CD33 monoclonal antibody conjugated with the cytotoxic antibiotic calicheamicin, and this side effect could be due to CD33 expression in normal HSCs (**Taussig et al., 2005**). CLL-1, CSF1R, TIM-3, and CD96 are the group of molecules that are specifically expressed in LSCs. Among all, the sensitivity of TIM-3 is likely to be the highest at least for AML M0, M1, M2, and M4 (Figures **1**B and **2**). Thus, TIM-3 might be one of the most useful therapeutic targets at least for these AML types.

It may also be important to understand function of these molecules in maintenance or reconstitution capability of LSCs. For example, it was shown that CD44 monoclonal antibodies reduced the leukemic burden and blocked secondary engraftment in a NOD-SCID model (**Jin et al., 2006**). This effect on LSCs was mediated in part by the disruption of LSC-niche interactions (**Jin et al., 2006**). CD47 antibodies can block LSC reconstitution and inhibited the growth of engrafted human AML in a NOD-SCID model (**Majeti et al., 2009**). However, the interpretation of this result is difficult because the anti-LSC effect of CD47 antibody treatment in this xenograft model could be due to induction of xenogeneic rejection by blocking the ligation of human CD47 expressed on LSCs with mouse SIRPA: NOD-type SIRPA expressed on host macrophage is agonistic for human CD47 to block phagocytotic signals, resulting in the induction of tolerance for human cells in this model (**Takenaka et al., 2007**). The effect of TIM-3 antibodies in our study might be due to killing activity for their target cells that should include LSCs. It is, however, still important to understand the role of TIM-3 signaling in LSC functions by, for example, testing the effect of activation or suppression of TIM-3 signaling on LSC fate decision.

In summary, TIM-3 is a promising surface molecule to target AML LSCs of most FAB types. Our in vivo experiments strongly suggest that targeting this molecule by monoclonal antibody treatment is a practical approach to eradicate human AML.

EXPERIMENTAL PROCEDURES

Clinical Samples

The bone marrow samples of 34 adult AML cases diagnosed according to French-American-British (FAB) and WHO criteria were enrolled. Human adult bone marrow and peripheral blood cells were obtained from healthy donors. Cord blood cells were obtained from full-term deliveries. Informed consent was obtained from all patients and controls in accordance with the Helsinki Declaration of 1975 that was revised in 1983. The Institutional Review Board of Kyushu University Hospital approved all research on human subjects.

Antibodies, Cell Staining, and Sorting

For the analyses and sorting of human HSCs and progenitors, cells were stained and sorted by FACS Aria (BD Biosciences) as we have previously reported (**Kikushige et al., 2008; Yoshimoto et al., 2009**). In brief, for the analyses and sorting of HSCs and myeloid progenitors, cells were stained with a Cy5-PE- or PC5-conjugated lineage cocktail, including anti-CD3 (HIT3a), CD4 (RPA-T4), CD8 (RPA-T8), CD10 (HI10a), CD19 (HIB19), CD20 (2H7), CD11b (ICFR44), CD14 (RMO52), CD56 (NKH-1), and GPA (GA-R2); FITC-conjugated anti-CD34 (8G12), anti-CD90 (5E10), or anti-CD45RA (HI100); PE-conjugated anti-TIM-3 (344823), CD33 (HIM3-4), CD96 (NK92.39), or anti-CD123 (6H6); APC-conjugated anti-CD34 (8G12) or anti-CD38 (HIT2); and Pacific Blue conjugated anti-CD45RA (HI100), and biotinylated anti-CD38 (HIT2), or anti-CD123 (9F5). For analysis and sorting of human cells in the immunodeficient mice, FITC-conjugated anti-CD33 (HIM3-4), PE-conjugated anti-CD19 (HIB19), PE-Cy7-conjugated anti-CD38 (HIT2), and APC-conjugated anti-CD45 (J.33) monoclonal antibodies were used in addition to the antibodies described above. Streptavidin-conjugated APC-Cy7 or PE-Cy7 was used for visualization of the biotinylated antibodies (BD PharMingen, San Jose, CA). Nonviable cells were excluded by propidium iodide (PI) staining. Appropriate isotype-matched, irrelevant control monoclonal antibodies were used to determine the level of background staining. The cells were sorted and analyzed by FACS Aria (BD Biosciences, San Jose, CA). The sorted cells were subjected to an additional round of sorting withthe same gate to eliminate contaminating cells and doublets. For single-cell assays, an automatic cell-deposition unit system (BD Biosciences, San Jose, CA) was used.

In Vitro Assays to Determine the Differentiation Potential of Myeloid Progenitors

Clonogenic colony-forming unit (CFU) assays were performed with a methylcellulose culture system that was set up to detect all possible outcomes of myeloid differentiation as reported previously (**Kikushige et al., 2008; Manz et al., 2002**). Colony numbers were enumerated on day 14 of culture. All of the cultures were incubated at 37°C in a humidified chamber under 5% CO_2.

Microarray Analysis

Twelve AML samples and five normal adult HSCs samples were investigated with Sentrix Bead Chip Assay For Gene Expression, Human-6 V2 (Illumina). In brief, total RNA was extracted with TRIzol (Invitrogen) from FACS-sorted AML $CD34^+CD38^-$ cells and normal $CD34^+CD38^-Lin^-$ HSCs, and biotinylated complementary RNA was synthesized with two round amplification steps via MessageAmpII aRNA Amplification Kit and Illumina TotalPrep RNA Amplification Kit (Applied Biosystems). 1.5 μg of cRNA from each sample was hybridized to the Bead Chip. After staining and washing, Bead Chip was scanned with an Illumina Bead Array reader. Microarray data were analyzed with Gene Spring GX11.01 software (Agilent Technologies). According to the guided workflow for Illumina single color experiment, normalization algorithm of 75-percentile shift was used, and the preprocessing baseline was adjusted to median of all samples.

Production of Recombinant Anti-Human TIM-3 Mouse Monoclonal Antibody

Human TIM-3 cDNA were cloned from normal pancreas cDNA (Clontech). Female Balb/C mouse (7-week-old, Purchased from Charles River) was immunized with L929 cells stably expressing TIM-3 four times and soluble human TIM-3 protein once. Four days after the final injection, spleen cells were fused with SP2/O cells by the PEG method and selected in the HAT-medium. Hybridomas were screened by FACS and clone-sorted. cDNAs encoding the variable regions amplified by SMART RACE cDNA Kit (Clontech) and specific primers (**Doenecke et al., 1997**) were ligated to mouse IgG2a or Igκ constant region.

Evaluation of ADCC and CDC Activities of ATIK2a Antibodies

ADCC and CDC were determined as previously described with slight modification (**Shields et al., 2001; Tawara et al., 2008**). For ADCC, target cells and IL-2-cultured peripheral blood mononuclear cells prepared from healthy volunteers were incubated with antibodies (1 μg/mL, Effecter/Target ratio = 25). Cytotoxicity was analyzed by CytoTox 96 Non-Radioactive Cytotoxicity Assay (Promega) as follows: specific lysis [%] = $(A_E - A_{Allo})/(A_{Max} - A_{TS}) \times 100$, where A_E is absorbance of experiment, A_{Allo} is allogenic reaction (no antibody control), A_{Max} is maximum, A_{TS} is target spontaneous release. For CDC, viability of target cells incubated with rabbit sera was assayed by CellTiterGlo (Promega, no antibody control = 100%). UPC 10 (Sigma) replaced in PBS was used as an isotype control.

Transplantation of AML Cells into Immunodeficient Mice

NOD-SCID and NRG mice (stock#7799) were purchased from The Jackson Laboratory. The mice were housed in a specific-pathogen-free facility in micro-isolator cages at the Kyushu University. Animal experiments were performed in accordance with institutional guidelines approved by the Kyushu University animal care committee. NOD-SCID and NRG mice were irradiated at a sublethal dose (2.4 Gy and 4.8 Gy, respectively). In transplantation of AML cells, NOD-SCID mice additionally received a single intraperitoneal injection of 200 μg purified CD122 antibodies that were generated from TM-β1 hybridoma (**Tanaka et al., 1993**) before transplantation, based on the expectation that it induces transient reduction of NK cells and helps human cell engraftment. We did not inject CD122 antibodies in transplantion of normal bone marrow or cord blood cells. AML cells or $CD34^+$ cells from adult bone marrow and cord blood cells were transplanted via a tail vein.

Statistical Analysis

Data were presented as the mean ± standard deviation. The significance of the differences between groups was determined via Student's t test.

ACCESSION NUMBERS

The microarray data are available in the Gene Expression Omnibus (GEO) database (**http://www.ncbi.nlm.nih.gov/gds**) under the accession number 24395.

SUPPLEMENTAL INFORMATION

Supplemental Information includes two tables and can be found with this article online at **doi:10.1016/j.stem.2010.11.014**.

ACKNOWLEDGMENTS

This work was supported in part by a Grant-in-Aid from the Ministry of Education, Culture, Sports, Science and Technology in Japan. S.-i.T. and Y.I. are employees of Kyowa Hakko Kirin Co., Ltd.

Received: February 25, 2010
Revised: August 23, 2010
Accepted: October 6, 2010
Published: December 2, 2010

REFERENCES

Aikawa, Y., Katsumoto, T., Zhang, P., Shima, H., Shino, M., Terui, K., Ito, E., Ohno, H., Stanley, E.R., Singh, H., et al. (2010). PU.1-mediated upregulation of CSF1R is crucial for leukemia stem cell potential induced by MOZ-TIF2. Nat. Med. *16*, 580–585, 1p, 585.

Anderson, A.C., Anderson, D.E., Bregoli, L., Hastings, W.D., Kassam, N., Lei, C., Chandwaskar, R., Karman, J., Su, E.W., Hirashima, M., et al. (2007). Promotion of tissue inflammation by the immune receptor Tim-3 expressed on innate immune cells. Science *318*, 1141–1143.

Bhatia, M., Wang, J.C., Kapp, U., Bonnet, D., and Dick, J.E. (1997). Purification of primitive human hematopoietic cells capable of repopulating immune-deficient mice. Proc. Natl. Acad. Sci. USA *94*, 5320–5325.

Bonnet, D., and Dick, J.E. (1997). Human acute myeloid leukemia is organized as a hierarchy that originates from a primitive hematopoietic cell. Nat. Med. *3*, 730–737.

Doenecke, A., Winnacker, E.L., and Hallek, M. (1997). Rapid amplification of cDNA ends (RACE) improves the PCR-based isolation of immunoglobulin variable region genes from murine and human lymphoma cells and cell lines. Leukemia *11*, 1787–1792.

Florian, S., Sonneck, K., Hauswirth, A.W., Krauth, M.T., Schernthaner, G.H., Sperr, W.R., and Valent, P. (2006). Detection of molecular targets on the surface of CD34+/CD38-/- stem cells in various myeloid malignancies. Leuk. Lymphoma *47*, 207–222.

Hauswirth, A.W., Florian, S., Printz, D., Sotlar, K., Krauth, M.T., Fritsch, G., Schernthaner, G.H., Wacheck, V., Selzer, E., Sperr, W.R., and Valent, P. (2007). Expression of the target receptor CD33 in CD34+/CD38-/CD123+ AML stem cells. Eur. J. Clin. Invest. *37*, 73–82.

Hope, K.J., Jin, L., and Dick, J.E. (2004). Acute myeloid leukemia originates from a hierarchy of leukemic stem cell classes that differ in self-renewal capacity. Nat. Immunol. *5*, 738–743.

Hosen, N., Park, C.Y., Tatsumi, N., Oji, Y., Sugiyama, H., Gramatzki, M., Krensky, A.M., and Weissman, I.L. (2007). CD96 is a leukemic stem cell-specific marker in human acute myeloid leukemia. Proc. Natl. Acad. Sci. USA *104*, 11008–11013.

Ishikawa, F., Yasukawa, M., Lyons, B., Yoshida, S., Miyamoto, T., Yoshimoto, G., Watanabe, T., Akashi, K., Shultz, L.D., and Harada, M. (2005). Development of functional human blood and immune systems in NOD/SCID/IL2 receptor gamma chain(null) mice. Blood *106*, 1565–1573.

Ishikawa, F., Yoshida, S., Saito, Y., Hijikata, A., Kitamura, H., Tanaka, S., Nakamura, R., Tanaka, T., Tomiyama, H., Saito, N., et al. (2007). Chemotherapy-resistant human AML stem cells home to and engraft within the bone-marrow endosteal region. Nat. Biotechnol. *25*, 1315–1321.

Jaiswal, S., Jamieson, C.H., Pang, W.W., Park, C.Y., Chao, M.P., Majeti, R., Traver, D., van Rooijen, N., and Weissman, I.L. (2009). CD47 is upregulated on circulating hematopoietic stem cells and leukemia cells to avoid phagocytosis. Cell *138*, 271–285.

Jin, L., Hope, K.J., Zhai, Q., Smadja-Joffe, F., and Dick, J.E. (2006). Targeting of CD44 eradicates human acute myeloid leukemic stem cells. Nat. Med. *12*, 1167–1174.

Jin, L., Lee, E.M., Ramshaw, H.S., Busfield, S.J., Peoppl, A.G., Wilkinson, L., Guthridge, M.A., Thomas, D., Barry, E.F., Boyd, A., et al. (2009). Monoclonal antibody-mediated targeting of CD123, IL-3 receptor alpha chain, eliminates human acute myeloid leukemic stem cells. Cell Stem Cell *5*, 31–42.

Kikushige, Y., Yoshimoto, G., Miyamoto, T., Iino, T., Mori, Y., Iwasaki, H., Niiro, H., Takenaka, K., Nagafuji, K., Harada, M., et al. (2008). Human Flt3 is expressed at the hematopoietic stem cell and the granulocyte/macrophage progenitor stages to maintain cell survival. J. Immunol. *180*, 7358–7367.

Krause, D.S., and Van Etten, R.A. (2007). Right on target: Eradicating leukemic stem cells. Trends Mol. Med. *13*, 470–481.

Lapidot, T., Sirard, C., Vormoor, J., Murdoch, B., Hoang, T., Caceres-Cortes, J., Minden, M., Paterson, B., Caligiuri, M.A., and Dick, J.E. (1994). A cell initiating human acute myeloid leukaemia after transplantation into SCID mice. Nature *367*, 645–648.

Majeti, R., Chao, M.P., Alizadeh, A.A., Pang, W.W., Jaiswal, S., Gibbs, K.D., Jr., van Rooijen, N., and Weissman, I.L. (2009). CD47 is an adverse prognostic factor and therapeutic antibody target on human acute myeloid leukemia stem cells. Cell *138*, 286–299.

Manz, M.G., Miyamoto, T., Akashi, K., and Weissman, I.L. (2002). Prospective isolation of human clonogenic common myeloid progenitors. Proc. Natl. Acad. Sci. USA *99*, 11872–11877.

Martelli, M.P., Pettirossi, V., Thiede, C., Bonifacio, E., Mezzasoma, F., Cecchini, D., Pacini, R., Tabarrini, A., Ciurnelli, R., Gionfriddo, I., et al. (2010). CD34+ cells from AML with mutated NPM1 harbor cytoplasmic mutated nucleophosmin and generate leukemia in immunocompromised mice. Blood Press. Published online July 15, 2010. 10.1182/blood-2009-08-238899.

Monney, L., Sabatos, C.A., Gaglia, J.L., Ryu, A., Waldner, H., Chernova, T., Manning, S., Greenfield, E.A., Coyle, A.J., Sobel, R.A., et al. (2002). Th1-specific cell surface protein Tim-3 regulates macrophage activation and severity of an autoimmune disease. Nature *415*, 536–541.

Nakae, S., Iikura, M., Suto, H., Akiba, H., Umetsu, D.T., Dekruyff, R.H., Saito, H., and Galli, S.J. (2007). TIM-1 and TIM-3 enhancement of Th2 cytokine production by mast cells. Blood *110*, 2565–2568.

Nakayama, M., Akiba, H., Takeda, K., Kojima, Y., Hashiguchi, M., Azuma, M., Yagita, H., and Okumura, K. (2009). Tim-3 mediates phagocytosis of apoptotic cells and cross-presentation. Blood *113*, 3821–3830.

Nimmerjahn, F., and Ravetch, J.V. (2005). Divergent immunoglobulin g subclass activity through selective Fc receptor binding. Science *310*, 1510–1512.

Nimmerjahn, F., and Ravetch, J.V. (2007). Antibodies, Fc receptors and cancer. Curr. Opin. Immunol. *19*, 239–245.

Pearson, T., Shultz, L.D., Miller, D., King, M., Laning, J., Fodor, W., Cuthbert, A., Burzenski, L., Gott, B., Lyons, B., et al. (2008). Non-obese diabetic-recombination activating gene-1 (NOD-Rag1 null) interleukin (IL)-2 receptor common gamma chain (IL2r gamma null) null mice: A radioresistant model for human lymphohaematopoietic engraftment. Clin. Exp. Immunol. *154*, 270–284.

Sabatos, C.A., Chakravarti, S., Cha, E., Schubart, A., Sánchez-Fueyo, A., Zheng, X.X., Coyle, A.J., Strom, T.B., Freeman, G.J., and Kuchroo, V.K. (2003). Interaction of Tim-3 and Tim-3 ligand regulates T helper type 1 responses and induction of peripheral tolerance. Nat. Immunol. *4*, 1102–1110.

Saito, Y., Kitamura, H., Hijikata, A., Tomizawa-Murasawa, M., Tanaka, S., Takagi, S., Uchida, N., Suzuki, N., Sone, A., Najima, Y., et al. (2010). Identification of therapeutic targets for quiescent, chemotherapy-resistant human leukemia stem cells. Sci. Transl. Med. 2, ra9.

Sánchez-Fueyo, A., Tian, J., Picarella, D., Domenig, C., Zheng, X.X., Sabatos, C.A., Manlongat, N., Bender, O., Kamradt, T., Kuchroo, V.K., et al. (2003). Tim-3 inhibits T helper type 1-mediated auto- and alloimmune responses and promotes immunological tolerance. Nat. Immunol. *4*, 1093–1101.

Shields, R.L., Namenuk, A.K., Hong, K., Meng, Y.G., Rae, J., Briggs, J., Xie, D., Lai, J., Stadlen, A., Li, B., et al. (2001). High resolution mapping of the binding site on human IgG1 for Fc gamma RI, Fc gamma RII, Fc gamma RIII, and FcRn and design of IgG1 variants with improved binding to the Fc gamma R. J. Biol. Chem. *276*, 6591–6604.

Takenaka, K., Prasolava, T.K., Wang, J.C., Mortin-Toth, S.M., Khalouei, S., Gan, O.I., Dick, J.E., and Danska, J.S. (2007). Polymorphism in Sirpa modulates engraftment of human hematopoietic stem cells. Nat. Immunol. *8*, 1313–1323.

Tanaka, T., Kitamura, F., Nagasaka, Y., Kuida, K., Suwa, H., and Miyasaka, M. (1993). Selective long-term elimination of natural killer cells in vivo by an anti-interleukin 2 receptor beta chain monoclonal antibody in mice. J. Exp. Med. *178*, 1103–1107.

Taussig, D.C., Pearce, D.J., Simpson, C., Rohatiner, A.Z., Lister, T.A., Kelly, G., Luongo, J.L., Danet-Desnoyers, G.A., and Bonnet, D. (2005). Hematopoietic stem cells express multiple myeloid markers: Implications for the origin and targeted therapy of acute myeloid leukemia. Blood *106*, 4086–4092.

Taussig, D.C., Miraki-Moud, F., Anjos-Afonso, F., Pearce, D.J., Allen, K., Ridler, C., Lillington, D., Oakervee, H., Cavenagh, J., Agrawal, S.G., et al. (2008). Anti-CD38 antibody-mediated clearance of human repopulating cells masks the heterogeneity of leukemia-initiating cells. Blood *112*, 568–575.

Taussig, D.C., Vargaftig, J., Miraki-Moud, F., Griessinger, E., Sharrock, K., Luke, T., Lillington, D., Oakervee, H., Cavenagh, J., Agrawal, S.G., et al. (2010). Leukemia-initiating cells from some acute myeloid leukemia patients with mutated nucleophosmin reside in the CD34(-) fraction. Blood *115*, 1976–1984.

Tawara, T., Hasegawa, K., Sugiura, Y., Harada, K., Miura, T., Hayashi, S., Tahara, T., Ishikawa, M., Yoshida, H., Kubo, K., et al. (2008). Complement activation plays a key role in antibody-induced infusion toxicity in monkeys and rats. J. Immunol. *180*, 2294–2298.

Uchida, J., Hamaguchi, Y., Oliver, J.A., Ravetch, J.V., Poe, J.C., Haas, K.M., and Tedder, T.F. (2004). The innate mononuclear phagocyte network depletes B lymphocytes through Fc receptor-dependent mechanisms during anti-CD20 antibody immunotherapy. J. Exp. Med. *199*, 1659–1669.

van Rhenen, A., van Dongen, G.A., Kelder, A., Rombouts, E.J., Feller, N., Moshaver, B., Stigter-van Walsum, M., Zweegman, S., Ossenkoppele, G.J., and Jan Schuurhuis, G. (2007). The novel AML stem cell associated antigen CLL-1 aids in discrimination between normal and leukemic stem cells. Blood *110*, 2659–2666.

Yalcintepe, L., Frankel, A.E., and Hogge, D.E. (2006). Expression of interleukin-3 receptor subunits on defined subpopulations of acute myeloid leukemia blasts predicts the cytotoxicity of diphtheria toxin interleukin-3 fusion protein against malignant progenitors that engraft in immunodeficient mice. Blood *108*, 3530–3537.

Yoshimoto, G., Miyamoto, T., Jabbarzadeh-Tabrizi, S., Iino, T., Rocnik, J.L., Kikushige, Y., Mori, Y., Shima, T., Iwasaki, H., Takenaka, K., et al. (2009). FLT3-ITD up-regulates MCL-1 to promote survival of stem cells in acute myeloid leukemia via FLT3-ITD-specific STAT5 activation. Blood *114*, 5034–5043.

Research article

Alloantigen expression on non-hematopoietic cells reduces graft-versus-leukemia effects in mice

Shoji Asakura,[1] Daigo Hashimoto,[1,2] Shuichiro Takashima,[3] Haruko Sugiyama,[1] Yoshinobu Maeda,[1] Koichi Akashi,[2,3] Mitsune Tanimoto,[1] and Takanori Teshima[2]

[1]Biopathological Science, Okayama University Graduate School of Medicine and Dentistry, Okayama, Japan. [2]Center for Cellular and Molecular Medicine and [3]Department of Medicine and Biosystemic Science, Kyushu University Graduate School of Science, Fukuoka, Japan.

Allogeneic hematopoietic stem cell transplantation (HSCT) is used effectively to treat a number of hematological malignancies. Its beneficial effects rely on donor-derived T cell–targeted leukemic cells, the so-called graft-versus-leukemia (GVL) effect. Induction of GVL is usually associated with concomitant development of graft-versus-host disease (GVHD), a major complication of allogeneic HSCT. The T cells that mediate GVL and GVHD are activated by alloantigen presented on host antigen-presenting cells of hematopoietic origin, and it is not well understood how alloantigen expression on non-hematopoietic cells affects GVL activity. Here we show, in mouse models of MHC-matched, minor histocompatibility antigen–mismatched bone marrow transplantation, that alloantigen expression on host epithelium drives donor T cells into apoptosis and dysfunction during GVHD, resulting in a loss of GVL activity. During GVHD, programmed death–1 (PD-1) and PD ligand–1 (PD-L1), molecules implicated in inducing T cell exhaustion, were upregulated on activated T cells and the target tissue, respectively, suggesting that the T cell defects driven by host epithelial alloantigen expression might be mediated by the PD-1/PD-L1 pathway. Consistent with this, blockade of PD-1/PD-L1 interactions partially restored T cell effector functions and improved GVL. These results elucidate a previously unrecognized significance of alloantigen expression on non-hematopoietic cells in GVL and suggest that separation of GVL from GVHD for more effective HSCT may be possible in human patients.

Introduction

Donor immunity in allogeneic hematopoietic stem cell transplantation (HSCT) harnesses beneficial graft-versus-leukemia (GVL) effects; therefore, allogeneic HSCT represents a very potent form of immunotherapy for hematological malignancies (1, 2). Induction of GVL is usually associated with the development of graft-versus-host disease (GVHD), which is a major complication after allogeneic HSCT. T cell depletion of the donor inocula prevents GVHD and leads to a loss of the GVL effect (3–5). Both GVL and GVHD are mediated by donor T cells, which recognize alloantigens presented on host APCs (6, 7). Donor CTLs and inflammatory cytokines are major effectors of GVHD, whereas CTLs are primarily responsible for GVL (8, 9). In patients with advanced-stage leukemia and lymphoma, relapse is still a major cause of mortality after allogeneic HSCT even after the development of severe GVHD. Thus, improvements in our understanding of the pathophysiology of GVHD and GVL are urgently needed to develop more effective therapies for malignant diseases.

Alloantigens are expressed on the three major components in HSCT recipients in the context of GVHD and GVL: hematopoietically derived APCs, GVHD target epithelium, and leukemia cells. Several studies have shown that host APCs are crucial for the induction of both GVHD and GVL (6, 7, 9–11). Alloantigen expression on epithelium is also critical for the induction of GVHD in MHC-matched, minor histocompatibility antigen–mismatched (mHA-mismatched) models of bone marrow transplantation (BMT) (10), but GVHD can occur in the absence of alloantigen expression on epithelium in MHC-mismatched models of BMT (9). However, the effect of alloantigen expression on non-hematopoietic cells such as the epithelium in GVL is not well defined. In this study, we addressed this important issue in mHA-mismatched models of BMT.

Results

Alloantigen expression on host non-hematopoietic cells augments acute GVHD but reduces GVL effects. We generated BM chimeric mice that express alloantigens on APCs, which are essential for the induction of both GVHD and GVL (6, 7, 12). BM chimeras were created by reconstituting lethally irradiated C3H.Sw (C3: H-2^b) mice with 5×10^6 T cell–depleted (TCD) BM cells isolated from C57BL/6 (B6, H-2^b) mice that differ from C3 mice at multiple mHAs ([B6→C3] chimeras). Control chimeras, [B6→B6], were identically created. Four months later, donor repopulation of hematopoiesis was confirmed by flow cytometry as shown previously (6, 9, 12). Thus, [B6→C3] chimeric mice expressed B6-derived mHAs on hematopoietically derived APCs but not on non-hematopoietic target cells. In contrast, [B6→B6] mice expressed B6-derived mHAs on both APCs and target epithelium. These chimeras were used as BMT recipients; they were reirradiated and injected with 5×10^6 TCD BM cells alone or with various doses of $CD8^+$ T cells from C3 donors. After BMT, GVHD mortality was higher in [B6→B6] mice than in [B6→C3] mice (Figure 1A). Clinical GVHD scores (13) in surviving animals were also higher in [B6→B6] mice than in [B6→C3] mice (Figure 1B). Mortality and morbidity from GVHD in [B6→C3] mice were almost equivalent to those in [B6→B6] mice given a 1-log lower T cell dose. This finding confirmed the previous observation of a lack of alloantigen expression on host epithelium significantly reducing GVHD across mHA disparity (10). We

Conflict of interest: The authors have declared that no conflict of interest.

Citation for this article: *J Clin Invest.* 2010;120(7):2370–2378. doi:10.1172/JCI39165.

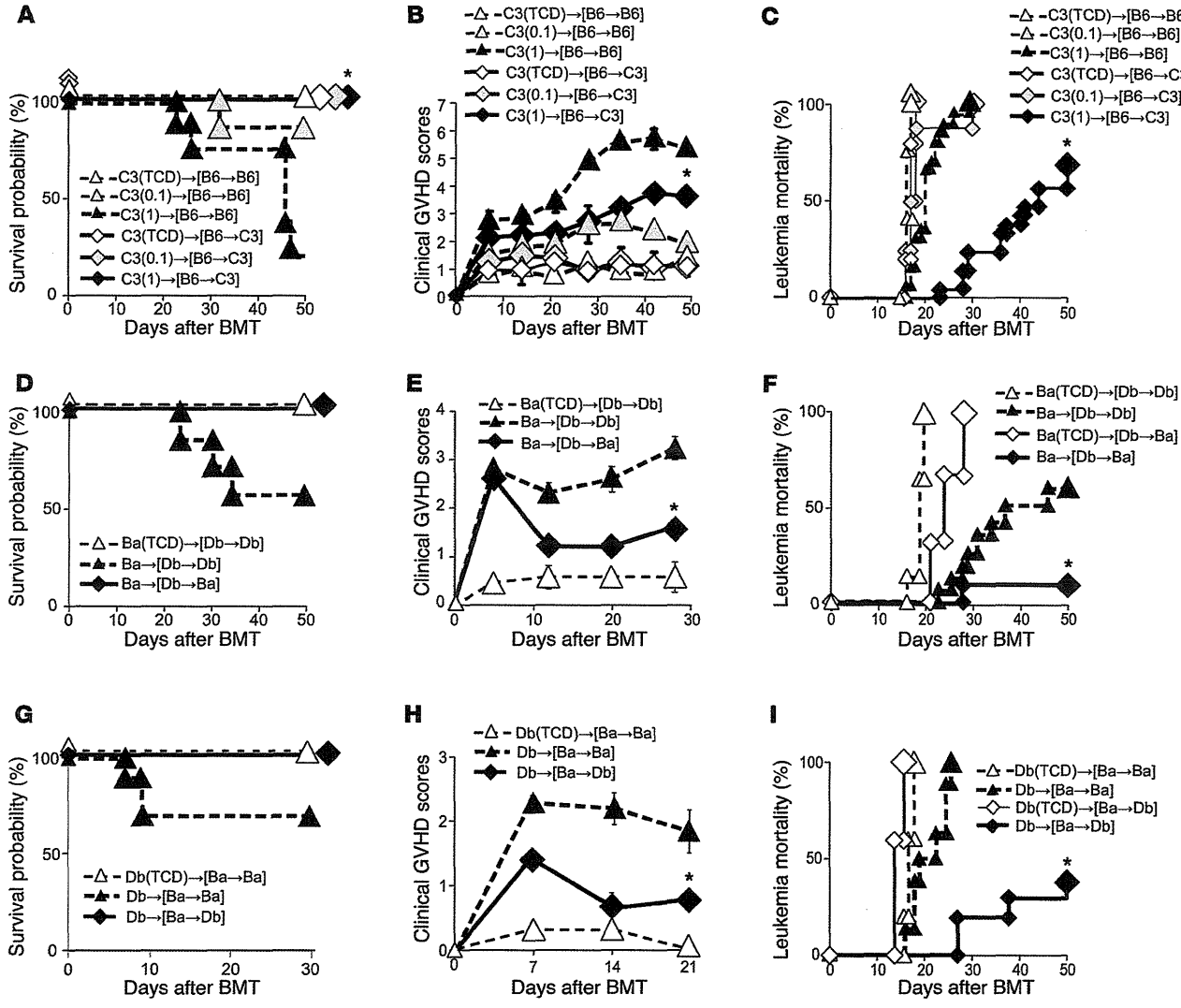

Figure 1

Alloantigen expression on host non-hematopoietic cells augments acute GVHD but reduces GVL effects. (**A–C**) [B6→C3] (diamonds) and [B6→B6] chimeras (triangles) were created by reconstituting lethally irradiated C3 and B6 mice with 5 × 10^6 TCD BM cells from B6 mice. Four months later, the chimeras were reirradiated and injected with 5 × 10^6 TCD BM cells alone (open symbols) or with 1 × 10^6 (black symbols) or 0.1 × 10^6 (gray symbols) $CD8^+$ T cells from C3 donors (as indicated in parentheses × 10^6). Survival (**A**) and clinical GVHD scores (**B**) after BMT (n = 3–8/group). (**C**) Leukemia mortality after BMT in chimeras injected with EL4 cells (n = 5–21/group). Data from 3 similar experiments were combined. (**D–F**) [Db→Ba] (diamonds) and [Db→Db] (triangles) chimeras were reirradiated and injected with TCD BM alone (open symbols) or with 2 × 10^6 T cells from Ba donors (filled symbols). Survival (**D**) and clinical GVHD scores (**E**) after BMT from a representative experiment of 2 similar experiments (n = 4–7/group). (**F**) Leukemia mortality after BMT in mice injected with P815 cells. Data from 2 similar experiments were combined (n = 6–18/group). (**G–I**) [Ba→Db] (diamonds) and [Ba→Ba] (triangles) chimeras were similarly transplanted with 5 × 10^6 TCD BM cells alone (open symbols) or with 2 × 10^6 T cells from Db donors (filled symbols). Survival (**G**) and clinical scores (**H**) after BMT (n = 3–10/group). (**I**) Leukemia mortality after BMT in chimeras injected with A20 cells (n = 5–10/group). Data from 2 similar experiments were combined. Clinical scores are shown as the mean ± SEM. *P < 0.05 compared with allogeneic controls.

then tested the effect of alloantigen expression on GVHD target epithelium on GVL effects. These chimeric mice were transplanted as described above together with 2,500 B6-derived EL4 cells as a model of residual leukemia after BMT. As expected, 100% of both types of chimeric mice that received TCD BM cells died from leukemia by day +20 after BMT (Figure 1C), whereas leukemia-free survival was significantly prolonged in mice that received donor T cells, demonstrating a significant GVL effect. However, this GVL effect was not potent in [B6→B6] mice, and all mice subsequently died from leukemia. Surprisingly, leukemia mortality was significantly lower in [B6→C3] mice that did not express alloantigens on their non-hematopoietic cells (62% vs. 100%; P < 0.05). GVL effects in [B6→B6] mice appeared to be almost equivalent to those in [B6→C3] mice given a 1-log lower T cell dose.

We further confirmed these observations in a different strain combination: BALB/c (Ba, H-2^d) and DBA/2 (Db, H-2^d) mice that

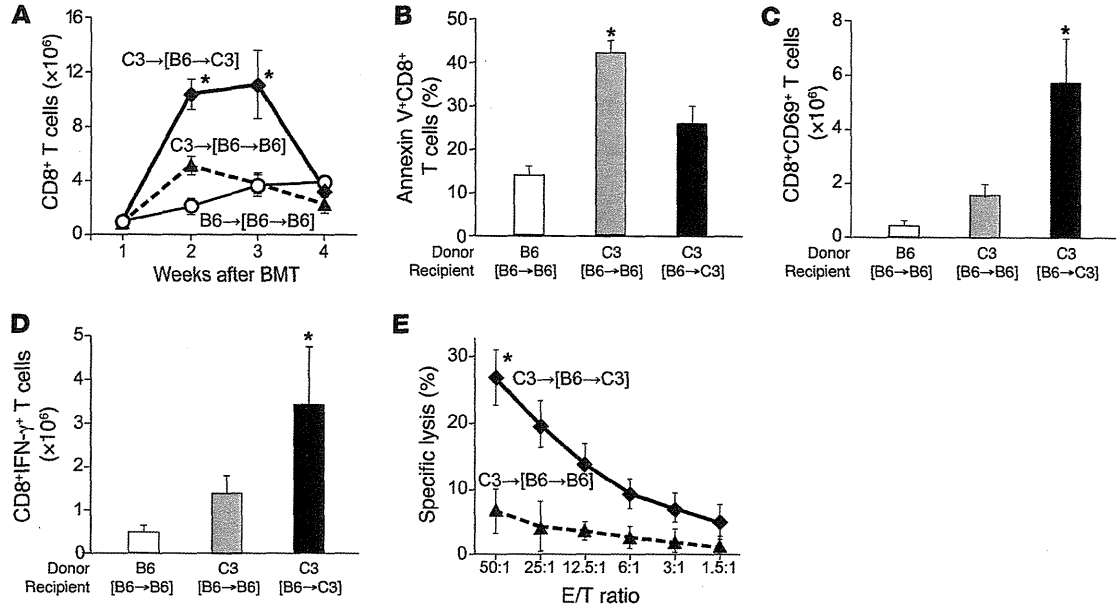

Figure 2

Alloantigen expression on host non-hematopoietic cells enhances the apoptosis and dysfunction of alloreactive T cells. [B6→C3] (diamonds and black bars) and [B6→B6] (triangles and gray bars) chimeras were transplanted as indicated in the legend for Figure 1. Syngeneic controls were [B6→B6] recipients of B6.Ly5.1 (CD45.1+) cells (open circles and white bars). (**A**) Numbers of donor CD8+ T cells in spleens. (**B**) Frequencies of annexin V+ donor CD8+ T cells. (**C**) Numbers of annexin V− donor CD69+CD8+ T cells. (**D**) Numbers of annexin V− IFN-γ–producing donor CD8+ T cells. (**E**) CTL activity against EL4. (**B–E**) Analysis was performed 14 days after BMT (n = 3–8/group). Representative data from 1 of the experiments are shown as the mean ± SD. *$P < 0.05$ compared with allogeneic controls.

differed at multiple mHAs from each other. [Db→Ba] and control [Db→Db] chimeras were lethally reirradiated and injected with 5 × 10^6 TCD BM cells alone or with 2 × 10^6 Ba T cells. Mortality (Figure 1D, $P = 0.08$) and morbidity from GVHD (Figure 1E, $P < 0.05$) were higher in [Db→Db] mice than in [Db→Ba] mice. When cells were transplanted together with 2,000 Db-derived P815 cells, leukemia mortality was significantly lower in [Db→Ba] mice than in [Db→Db] mice (10% vs. 60%; $P < 0.05$) (Figure 1F).

Similar results were obtained when [Ba→Db] and control [Ba→Ba] chimeras were transplanted with 5 × 10^6 TCD BM cells with or without 2 × 10^6 Db T cells. In [Ba→Db] recipients, in which non-hematopoietic cells do not express alloantigens, mortality (Figure 1G, $P = 0.08$) and morbidity of GVHD (Figure 1H, $P < 0.05$) were lower, but GVL effects against Ba-derived A20 lymphoma cells were significantly more potent as compared with [Ba→Ba] controls (leukemia mortality: 30% vs. 100%; $P < 0.05$) (Figure 1I). Taken together, these results demonstrate that GVHD is decreased but GVL activity is enhanced in the absence of alloantigen expression on non-hematopoietic cells.

Alloantigen expression on non-hematopoietic cells enhances apoptosis and dysfunction of alloreactive T cells. GVHD and GVL in the C3 and B6 strain combination is dependent on donor CD8+ T cells (12, 14). To elucidate the mechanisms responsible for the enhancement of the GVL effect in [B6→C3] chimeric mice, which lack alloantigen expression on non-hematopoietic cells, the kinetics of donor CD8+ T cell expansion and activation were evaluated after BMT. Expansion of donor CD8+ T cells identified as CD5.1+CD8+ cells peaked on day +14 in the spleens of allogeneic [B6→B6] recipients and decreased thereafter (Figure 2A), as previously shown in this model (15). CD8 expansion was significantly greater in [B6→C3] mice than in [B6→B6] mice on days +14 and +21. We next assessed donor T cell apoptosis as a determinant of the kinetics of T cell expansion. Frequencies of annexin V+ apoptotic donor CD8+ T cells were significantly greater in the spleen of [B6→B6] mice as compared with that of [B6→C3] mice on day +14 (Figure 2B). Notably, surviving donor CD8+ T cells were significantly less activated in [B6→B6] mice than in [B6→C3] mice when evaluated based on the expression of CD69 (Figure 2C) and intracellular IFN-γ (Figure 2D) on annexin V− donor CD8+ T cells. We next evaluated CTL activity in donor T cells isolated from the spleen on day +14 after BMT. CTL activity against EL4 targets was significantly reduced in the splenocytes of [B6→B6] mice as compared with [B6→C3] mice (Figure 2E). These results suggest that alloantigen expression on non-hematopoietic cells induces apoptosis and dysfunction of alloreactive T cells.

Absence of alloantigen expression on host non-hematopoietic cells restores GVL effects. Self-recognition in the periphery facilitates the reactivity of mature T cells to foreign antigens (16). Therefore, it is possible that the expression of syngeneic MHC molecules and not the absence of alloantigens on non-hematopoietic cells may be responsible for the enhancement of the GVL effect in [B6→C3] chimeras. This possibility was tested in B6-background $\beta_2m^{-/-}$ mice. [B6→$\beta_2m^{-/-}$] chimeras lacking functional MHC class I molecules on non-hematopoietic cells did not develop GVHD after transplantation with CD8+ T cells from C3 donors, as shown previously (17) (Figure 3A). In these mice, however, leukemia mortality was significantly delayed even in the absence of GVHD as compared with [B6→B6] recipients (Figure 3B, $P < 0.05$). The expansion and CTL activity of donor CD8+ T cells was significantly greater in [B6→$\beta_2m^{-/-}$] recipients than in [B6→B6] recipients (Figure 3, C and D).

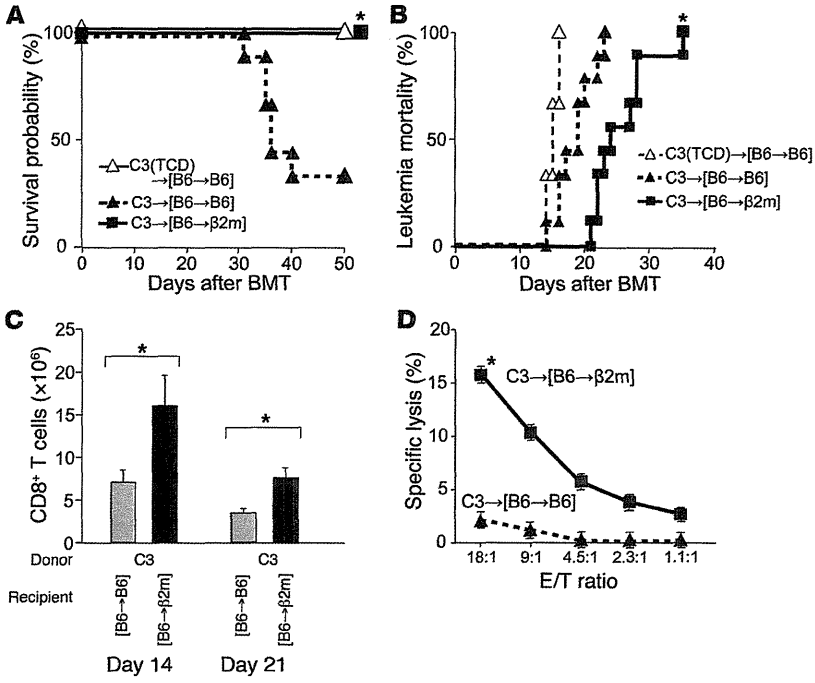

Figure 3
Absence of alloantigen expression on host nonhematopoietic cells restores GVL effects. [B6→B6] (triangles) and [B6→β2m$^{-/-}$] (squares) mice were reirradiated and injected with 5 × 10^6 TCD BM cells alone (open symbols) or with 1 × 10^6 CD8$^+$ T cells from C3 donors (filled symbols). (**A**) Survival after BMT. (**B**) Leukemia mortality in chimeras injected with EL4 cells (n = 6–9/group). Data from a representative experiment of 2 similar experiments are shown. Mean ± SEM numbers of donor CD8$^+$ T cells in spleens (n = 3–6/group) (**C**) and CTL activity against EL4 (**D**). *P < 0.05 compared with allogeneic controls.

These results confirm that alloantigen expression on host epithelium induces apoptosis and dysfunction of alloreactive T cells, which results in impaired GVL effects.

Alloantigen expression on host non-hematopoietic cells stimulates programmed death-1 and its ligand pathway. Programmed death-1 (PD-1) is a negative regulator of activated T cells and regulates T cell exhaustion during chronic infections (18–20). PD-1 interacts with at least 2 ligands: PD ligand-1 (PD-L1) and PD-L2 (21). In particular, the PD-1/PD-L1 pathway has been proposed as one of the most important mechanisms of T cell exhaustion and tolerance induction against infectious agents and tumors (19, 22–25). We therefore hypothesized that the PD-1/PD-L1 pathway plays a role in the loss of GVL effects in [B6→B6] mice. To test this hypothesis, we examined PD-1 expression on donor CD8$^+$ T cells in lymph nodes on day +14 and +21 after BMT. It was significantly upregulated in allogeneic [B6→B6] recipients as compared with syngeneic controls but was low in [B6→C3] mice (Figure 4, A and B). We also investigated the expression of another inhibitory receptor, CTLA-4, on donor CD8$^+$ T cells. Although the expression of cytoplasmic CTLA-4 was slightly upregulated in allogeneic animals as compared with syngeneic animals, its level did not differ between [B6→B6] and [B6→C3] mice (5.5% ± 1.0% vs. 4.5% ± 0.2%, respectively; P = 0.50).

We next examined PD-L1 expression in the liver by real-time PCR after BMT. PD-L1 expression was markedly upregulated in the liver of allogeneic controls as compared with syngeneic controls (Figure 4C). In allogeneic [B6→C3] mice, it was slightly upregulated on day +14 but not on day +21. Immunohistochemical analysis confirmed upregulated expression of PD-L1 in the liver of [B6→B6] mice, as previously reported (Figure 4D) (21, 26). These results showed that alloantigen expression on GVHD target epithelium is associated with upregulation of the PD-1/PD-L1 interactions between donor T cells and GVHD target tissue.

Blockade of the interaction between PD-1 and PD-L1 enhances GVL activity. We next examined whether blocking the PD-1/PD-L1 pathway could enhance GVL activity. [B6→C3] and [B6→B6] chimeras were reirradiated and injected with TCD BM cells and CD8$^+$ T cells from C3 donors. Mice were i.p. injected with 500 μg of anti-PD-L1 mAb on day 0 and then with 200 μg on days +3, +6, +9, +12, +15, and +18 after BMT. In [B6→B6] recipients, injection of anti-PD-L1 mAbs significantly restored T cell functions on day +14, as assessed by CD69 expression (Figure 5A), IFN-γ production (Figure 5B), and CTL activity (Figure 5C). In [B6→C3] mice, it marginally upregulated CD69 expression, IFN-γ production, and CTL activity, although differences were not statistically significant (Figure 5, A, B, and D). As a consequence, anti-PD-L1 mAb administration significantly increased the severity of GVHD in [B6→B6] mice (Figure 5E) but not in [B6→C3] mice (Figure 5F). PD-L1 blockade also significantly augmented GVL activity in [B6→B6] recipients injected with EL4 cells on day 0 (Figure 5G, P < 0.05). It also delayed leukemia death in [B6→C3] mice, although the difference was not statistically significant (Figure 5H, P = 0.38). In controls, PD-L1 blockade did not affect leukemia mortality in TCD-BMT recipients (Figure 5H) or [B6→B6] recipients of syngeneic B6 CD8$^+$ T cells (data not shown).

Discussion

Alloantigens are expressed in three major sites in HSCT recipients: APCs, GVHD target epithelium, and leukemia cells. Alloantigen expression on APCs is essential for the induction of GVHD (6), and an optimal GVL response occurs when alloantigens are expressed on both host APCs and tumor cells (7). Alloantigen expression on the epithelium is also critical for the induction of GVHD across mHA disparities (10), but GVHD can occur in the absence of alloantigen expression on epithelium in MHC-mismatched BMT (9). In this study, we addressed the effect of alloantigen expression on target epithelium in GVL using chimeric mouse models of GVHD and GVL across mHA disparities. Our models mimic clinical BMT in patients not in remission, since most of the mice relapsed after allogeneic BMT. This high tumor burden enabled us to compare the magnitude of GVL activity in our models, and we made sur-

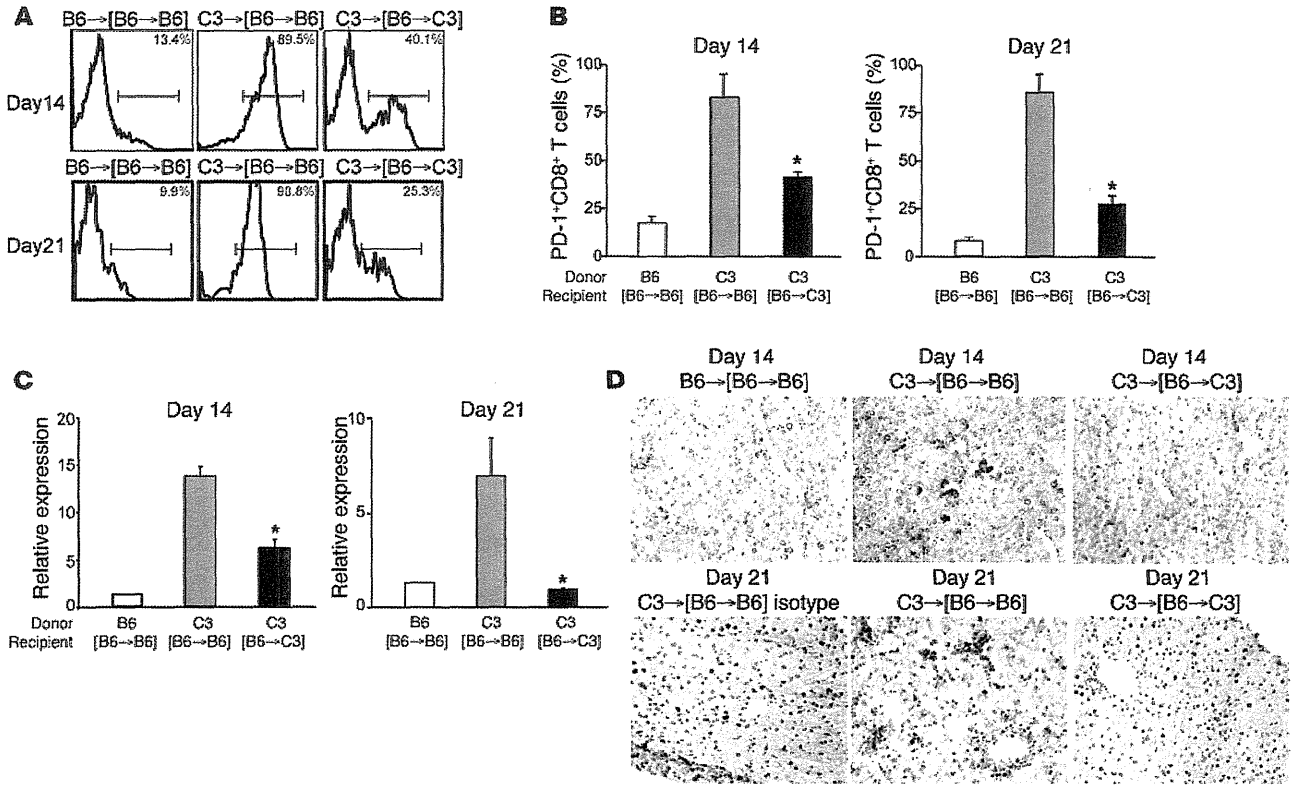

Figure 4

Alloantigen expression on host non-hematopoietic cells stimulates PD-1 and its ligand pathway. [B6→B6] and [B6→C3] chimeras were transplanted as indicated in the legend for Figure 1 (n = 4–8). (**A**) Representative histogram of PD-1 expression among donor CD8+ T cells on day +14 and +21 in syngeneic (left), allogeneic [B6→B6] (middle), and [B6→C3] (right) recipients. (**B**) Frequencies of PD-1+ CD8+ T cells (mean ± SD). (**C**) Relative expressions of *Pdl1* mRNA on day +14 and +21 in the livers of allogeneic [B6→B6] (gray bars) and allogeneic [B6→C3] mice (black bars). Data represent the mean (± SD) of n-fold difference in the amount of *Pdl1* gene expression relative to that in syngeneic mice. (**D**) PD-L1 expression in the liver on day +14 (top row) and +21 (bottom row) from syngeneic (upper left) and allogeneic [B6→B6] (middle) and [B6→C3] (right) recipients. Isotype control of allogeneic [B6→B6] (lower left) is shown. Original magnification, ×200. *$P < 0.05$ compared with allogeneic controls.

prising observations that alloantigen expression on non-hematopoietic cells inhibited GVL effects but enhanced GVHD. This observation challenges the current paradigm that GVL activity is strongly correlated with the severity of GVHD (1, 2, 27).

We found that alloantigen expression on non-hematopoietic cells induced donor T cell apoptosis and led to a contraction in the size of an alloreactive donor CD8+ T cell pool early after BMT. The remainder of the donor T cells were alive, but their ability to produce cytokines and cytotoxicity were impaired. This defect is similar to T cell exhaustion, which is a principal reason for the inability of the host to eliminate the persisting pathogen in chronic infections (18, 28). CD8+ T cell proliferation and differentiation into cytolytic effectors on an encounter with antigens are variable and change as a consequence of the antigen load (29). As the magnitude of the viral load increases, virus-specific T cells become more functionally impaired. During persistent infection, a high antigen load drives a significant number of virus-specific T cells into activation-induced apoptosis, and the remaining virus-specific T cells remain alive but in a dysfunctional state of cytotoxicity (18, 30–33). In tumor models, antigen quantity determines the behavior of the CD8+ effector cells, including their effector function and sensitivity to apoptosis (34–36). In patients with a larger tumor burden, CD8+ T cells were found to undergo apoptosis (37). Thus, a higher alloantigen load in allogeneic controls as compared with chimeras, in which alloantigen expression is limited to hematopoietic cells and tumor cells, may induce apoptosis and the dysfunction of alloreactive T cells, which leads to the inability of the host to eliminate leukemia.

Our results are consistent with seminal observations by Meunier, Fontaine, and colleagues, who showed that the adoptive transfer of immunodominant mHA ($B6^{dom1}$)–specific T cells eradicates $B6^{dom1}$-expressing leukemia more efficiently in mice lacking $B6^{dom1}$ expression than in mice expressing $B6^{dom1}$ (38). This was because the widespread expression of $B6^{dom1}$ caused activation-induced apoptosis and dysfunction of donor T cells in mice expressing $B6^{dom1}$ (38, 39). These findings along with our results indicate that allogeneic cellular therapy targeting mHAs exclusively expressed on APCs and tumor cells can induce a potent GVL effect while inducing less-severe GVHD than immunotherapy via targeting of ubiquitously expressed mHAs (40).

The PD-1/PD-L1 pathway is critically involved in T cell exhaustion and tolerance induction in infection and tumor immunology (18–20, 23–25, 41). It is also required for protection against chronic rejection of cardiac allograft, and induction of peripheral dele-

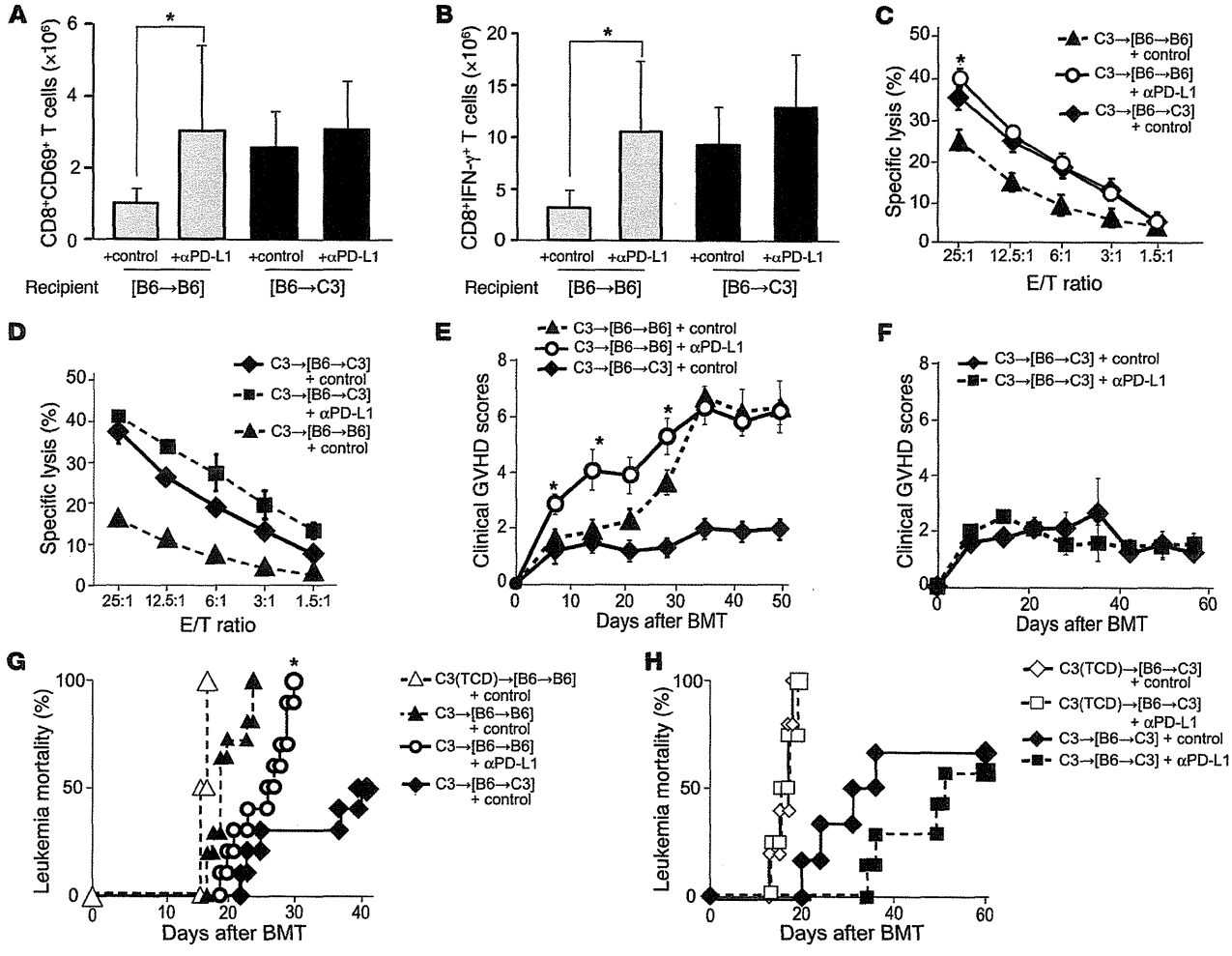

Figure 5

Blockade of the interaction between PD-1 and PD-L1 enhances GVL activity. [B6→C3] and [B6→B6] chimeras were reirradiated and injected with 5 × 10^6 TCD BM cells alone or with 1 × 10^6 $CD8^+$ T cells from C3 donors. Mice were i.p. injected with 500 μg of anti PD-L1 mAbs or controls on day 0 and then 200 μg thereafter on days +3, +6, +9, +12, +15, and +18. Splenocytes were harvested on day +14 to determine the number of $CD8^+CD69^+$ T cells (**A**) and IFN-γ–producing $CD8^+$ T cells (**B**) and CTL activity against EL4 targets (**C** and **D**). Results from a representative experiment of 2 similar experiments (means ± SD, n = 7–8/group). Mean clinical GVHD scores (±SEM) (**E** and **F**) after BMT are shown (n = 5–7/group). (**G** and **H**) Leukemia mortality after BMT in [B6→B6] and [B6→C3] chimeras injected with EL4 cells on day 0 (n = 4–11/group). Data from two similar experiments were combined. αPD-L1, anti–PD-L1 mAbs. *P < 0.05 compared with the corresponding controls.

tional tolerance of alloreactive, anti-donor $CD8^+$ T cells to achieve successful engraftment in BMT (42, 43). In this study, we found that PD-1 expression was upregulated in donor T cells and PD-L1 expression was upregulated in GVHD target organs. The expression of PD-1/PD-L1 was markedly reduced in chimeras lacking alloantigen expression on non-hematopoietic cells. PD-1 and PD-L1 expression is induced upon cell activation and inflammation in GVHD (44); therefore, the absence of alloantigen expression on GVHD target epithelium reduced GVHD in chimeric mice, which resulted in insufficient stimulation of the PD-1/PD-L1 interaction. Target tissue expression of PD-L1 is also critical for the induction of T cell exhaustion or tolerance in chronic viral infection, autoimmune diabetes, and cardiac allografting (19, 42, 45).

Both PD-1 and PD-L1 were markedly upregulated in [B6→B6] mice, but they were also modestly upregulated in [B6→C3] mice. Blockade of PD-1/PD-L1 interactions significantly restored T cell effector functions in [B6→B6] mice but modestly restored them in [B6→C3] mice as well. The relevance of these observations is shown by the PD-1/PD-L1 blockade studies. These data showed that the PD-1/PD-L1 pathway is particularly germane to [B6→B6] mice with widespread expression of alloantigens but also applies, at least in part, to [B6→C3] mice, wherein alloantigen expression is only on APCs. While there is likely to be a role for this pathway in the absence of epithelial alloantigen expression, the full negative impact of this pathway on GVL is only seen when alloantigen expression is present on non-hematopoietic tissues.

Of note, the improvement in GVL by the PD-1/PD-L1 blockade was partial, as has been shown in chronic viral infection (46–48). This may be due to the presence of multiple negative regulatory pathways that contribute to T cell exhaustion, including CTLA-4, IL-10, LAG-3, CD160, and 2B4 (20, 47, 49). In addition, the population of exhausted T cells is heterogeneous, and this interven-

tion is effective only for PD-1^{lo} and not PD-1^{hi}, which are subsets of exhausted T cells (50). Many of these inhibitory receptors are either coexpressed by the same exhausted T cells or differentially expressed on different subsets of exhausted cells. As the severity of the infection increases, the number of different inhibitors expressed per cell increases (47). A second inhibitory receptor, CTLA-4, can be overexpressed by exhausted CD4$^+$ T cells in chronic viral infection, but it appears to have a minimal role on exhausted CD8$^+$ T cells (19, 51). Although CTLA-4 was only slightly upregulated on CD8$^+$ T cells in contrast to the marked upregulation of PD-1 in our CD8-dependent model of MHC-matched BMT, the precise inhibitory receptors of therapeutic interest may differ between CD4$^+$-dependent and CD8$^+$-dependent GVHD/GVL. Another key negative regulatory pathway is mediated by Foxp3$^+$ Tregs. However, enhancement of GVL is not due to effects of the PD-1/PD-L1 blockade on Tregs, because blockade of PD-1/PD-L1 interactions enhances the expansion and function of Tregs (52). The hierarchy of these pathways in regulating GVL will need to be studied in the future based on better understanding of the delineation of T cell subsets and models (53). However, our results suggest the detrimental effect of GVHD-induced immunosuppression on GVL responses, regardless of which inhibitory pathway might be dominant clinically.

In addition, the administration of anti–PD-L1 mAb also exacerbated acute GVHD, as has been shown in a previous study (54). Therefore, the beneficial effects of the PD-1/PD-L1 blockade may be offset by the exacerbation of GVHD. Effects of the inhibitory receptor blockade might depend on the magnitude or stage of donor T cell activation and the severity of GVHD; therefore, the timing and duration of the targeting may be important.

In clinical HSCT, alloantigens continue to be presented on MHC class I in non-hematopoietic cells throughout the lifetime of the transplant recipients. However, a substantial number of patients eventually develop tolerance after resolution of GVHD and often experience leukemia relapse. Although activation-induced apoptosis of alloreactive T cells has been proposed as an explanation of this paradox (55), studies monitoring GVHD-specific T cell clones indicate that host-reactive T cells are continuously present after allogeneic HSCT (56–58). Our results provide a logical explanation for this paradox. However, the process of exhaustion is unlikely to occur in patients not developing GVHD, because induction of T cell exhaustion requires antigen-specific activation of T cells and subsequent differentiation into effector T cells. In these patients, tolerance could be induced by other mechanisms, such as functional central and peripheral tolerance mechanisms. It is well known that GVL is not apparent in patients with high leukemia burden. Although leukemia cells used in the current study do not express PD-L1 (22, 59), leukemia cells expressing PD-L1 may also directly limit the GVL response in patients with high leukemia burden (22, 24, 25). However, such insights from animal models must be extrapolated with caution to clinical studies involving humans.

It has been assumed that T cell exhaustion is antigen specific in chronic viral infection. Bystander lysis of T cells has also been reported in the course of viral infections (60), but is of minimal significance because of its limited magnitude and because normal thymic function can replenish the peripheral T cell pool. In contrast, in GVHD, T cell exhaustion occurs after initial T cell activation and the subsequent development of GVHD. GVHD induces bystander apoptosis of non-host-reactive T cells. In addition, GVHD-mediated injury of the thymus and the secondary lymphoid organs inhibits full replenishment of the peripheral T cell pool (55). Thus, establishment of full immune competence probably requires the additional process of T cell reconstitution following T cell exhaustion.

In conclusion, our results indicated the significance of alloantigen expression on non-hematopoietic cells in GVL. Alloantigen expression on non-hematopoietic cells induces the apoptosis of donor T cells and the dysfunction of cytotoxic effector function, which leads to a reduction in GVL activity. T cell dysfunction was partially restored by blocking PD-1/PD-L1 interactions, which suggests that the therapeutic "tuning" of T cell responses via modulation of negative regulatory pathways represents a novel strategy for enhancing GVL. Our results in combination with those of previous studies (6, 7, 9, 10, 38, 39) provide a complete picture of the effect of alloantigen expression on host APCs, GVHD target epithelium, and tumor cells in allogeneic HSCT; alloantigen expression on host non-hematopoietic cells augments GVHD but suppresses GVL effects. This concept may provide an important framework for understanding the pathophysiology of GVHD and allow for the separation of GVHD and GVL.

Methods

Mice. Female C57BL/6 (B6, H-2^b, CD45.2$^+$), BALB/c (Ba, H-2^d), and DBA/2 (Db, H-2^d) mice were purchased from Charles River Japan. B6.Ly5.1 (H-2^b, CD45.1$^+$) and C3H.Sw (C3, H-2^b) mice were purchased from The Jackson Laboratory. B6-background β_2m-deficient mice ($\beta_2m^{-/-}$: B6.129-β_2-m^{tm1Jae}N12) were purchased from Taconic. The age of mice used ranged from 8 to 12 weeks. Mice were maintained in specific pathogen–free conditions and received normal chaw and hyperchlorinated drinking water for the first 3 weeks after BMT. All experiments involving animals were performed according to a protocol approved by the Institutional Animal Care and Research Advisory Committee of Okayama University and Kyushu University.

Generation of bone marrow chimera and induction of GVHD and GVL. Total body irradiation (TBI: X-ray) was split into 2 doses separated by 4 hours to minimize gastrointestinal toxicity. B6 and C3 mice received 10 Gy TBI, whereas Ba and Db mice received 8.5 Gy TBI. To create BM chimeras, lethally irradiated mice were intravenously injected with 5 × 10^6 TCD BM cells from donors. TCD was performed using anti-CD90 microbeads and AutoMACS (Miltenyi Biotec). Four months later, the chimeric mice were reirradiated and injected with 5 × 10^6 TCD BM cells plus various doses of CD8$^+$ T cells or 2 × 10^6 T cells. T cells and CD8$^+$ T cells were negatively isolated from splenocytes by using a T cell isolation kit and a CD8$^+$ T cell isolation kit (Miltenyi Biotec), respectively, and the AutoMACS. In the GVL experiments, EL4 (H-2^b) derived from a B6 mouse, P815 (H-2^d) derived from a Db mouse, and A20 (H-2^d) derived from a Ba mouse were intravenously injected into BMT recipients on day 0 of BMT. Anti–PD-L1 mAbs were purified from the hybridoma supernatant of clone MIH5 (61), which was a gift from Miyuki Azuma of Tokyo Medical and Dental University, Tokyo, Japan, and i.p. injected at a dose of 500 μg/mouse on day 0, followed by 200 μg/mouse on days +3, +6, +9, +12, +15, and +18 after BMT.

Assessment of GVHD and GVL effects. Survival after BMT was monitored daily, and the degree of clinical GVHD was assessed weekly by using a scoring system that sums changes in 5 clinical parameters: weight loss, posture, activity, fur texture, and skin integrity (maximum index, 10) as described previously (13). The cause of each death after BMT was determined by post mortem examination, and was either GVHD or tumor. The most striking leukemia-specific abnormality induced by EL4, P815, and A20 was macroscopic tumor nodules, marked hepatosplenomegaly, and lower limb paralysis (62). Leukemia death induced by EL4, P815, and A20 was therefore defined by the occurrence of hepatosplenomegaly, macroscopic tumor nodules in the liver

and/or spleen, or hind leg paralysis. GVHD death was defined as the absence of leukemia and by the presence of clinical signs of GVHD, assessed by using a clinical scoring system. Animals surviving beyond the observation period of BMT were sacrificed, and the spleen and liver were harvested for histological evaluation to determine leukemia-free survival.

Flow cytometric analysis. The mAbs used were FITC-, PE-, PerCP-, Cy5.5-, or APC-conjugated anti–mouse CD5.1, CD8, CD45.1, CD45.2, CD69, and PD-1 (BD Biosciences). Cells positive for 7-amino-actinomycin D (BD Biosciences) were excluded from the analysis. For the analysis of donor T cell apoptosis, the cells were stained with Annexin V (MBL). For intracellular IFN-γ staining, the splenocytes were incubated for 4 hours with leukocyte activation cocktail and BD GolgiPlug (BD Biosciences) at 37°C. Then, the cells underwent permeabilization with a BD Cytofix/Cytoperm solution (BD Biosciences) and were stained with FITC-conjugated anti–IFN-γ mAbs (BD Biosciences). For intracellular CTLA-4 staining, cells were stained with PE-conjugated anti–CTLA-4 mAbs (eBioscience). At least 5,000 live events were acquired for the analysis using a FACSCalibur flow cytometer (BD Biosciences).

CTL assay. Splenocytes were removed from chimeric recipients 14 days after BMT, and the mononuclear cells were then separated by density gradient centrifugation. The percentage of $CD8^+$ cells in this fraction was determined by flow cytometry, and counts were normalized for $CD8^+$ cell numbers. Tumor targets, 2×10^6 P815 or EL4, were labeled with 100 μCi of ^{51}Cr sodium salt (Amersham Biosciences) for 2 hours. After washing 3 times, the labeled targets were resuspended in 10% FCS in RPMI and plated at 10^4 cells per well in U-bottom plates (Corning-Costar Corp.). Allogeneic splenocyte preparations, as described above, were added to quadruplicate wells at varying effector-to-target ratios and incubated for 4 hours. Maximal and background release were determined by adding 1% SDS and media alone to the targets, respectively. ^{51}Cr activity in the supernatants collected 4 hours later was determined using a Wallac 1470 WIZARD Gamma Counter (Wallac Oy), and lysis was expressed as a percentage of maximum: percentage of specific lysis = 100 (sample count − background count/maximum count − background count).

Quantitative real-time PCR. Total RNA was isolated from the frozen liver using ISOGEN (Nippon Gene). cDNA was synthesized from 150 μg RNA using a QuantiTect Reverse Transcription Kit (QIAGEN). *Pdl1* mRNA levels were quantified by real-time PCR using the 7500 Real-Time PCR System (Applied Biosystems). TaqMan Universal PCR MasterMix, primers, and the fluorescent TaqMan probe specific for murine PD-L1 (Mm00452054-m1) and a house keeping gene, mGAPDH (Mm99999915-g1), were purchased from Applied Biosystems. The standard was obtained using RNA extracted from syngeneic controls.

Immunohistochemistry. For immunohistochemical analysis, isolated livers were frozen in Tissue-Tek (Sakura Finetek), and 5-μm cryostat sections were prepared. Slides were fixed in 100% acetone and air dried. Endogenous peroxidase activity was blocked with peroxidase blocking reagent (Dako). The sections were incubated with purified rat anti–mouse PD-L1 mAb (clone MIH5; eBiosciences). The primary Abs were detected using the Histofine Simple Stain Mouse MAX PO (Rat) kit and DAB solution (Nichirei). The images were captured using an Olympus BH2 microscope with a Nikon DS-5M color digital camera (Nikon), controlled by Nikon ATC-2U software version 1.5. An Olympus ×10/20 ocular lens and a ×20/0.46 NA objective lens were used. Images were cropped using Adobe Photoshop (Adobe Systems) and were composed using Adobe Illustrator.

Statistics. We used the Kaplan-Meier product-limit method to obtain survival probability and the log-rank test to compare survival curves. The Mann-Whitney *U* test was used to analyze the clinical scores. A *P* value less than 0.05 was considered statistically significant.

Acknowledgments

We thank Miyuki Azuma of Tokyo Medical and Dental University for providing hybridoma MIH5-producing anti–PD-L1 mAbs. This study was supported by grant 21390295 from the Ministry of Education, Culture, Sports, Science, and Technology (Tokyo, Japan) (to T. Teshima), Health and Labor Science Research Grants (Tokyo, Japan) (to T. Teshima), and a grant from the Foundation for Promotion of Cancer Research (Tokyo, Japan) (to T. Teshima).

Received for publication March 11, 2009, and accepted in revised form April 7, 2010.

Address correspondence to: Takanori Teshima, Center for Cellular and Molecular Medicine, Kyushu University Hospital, 3-1-1 Maidashi, Higashi-ku, Fukuoka 812-8582, Japan. Phone: 81.92.642.5947; Fax: 81.92.642.5951; E-mail: tteshima@cancer.med.kyushu-u.ac.jp.

1. Weiden P, et al. Antileukemic effect of graft-versus-host disease in human recipients of allogeneic-marrow grafts. *N Engl J Med.* 1979;300(19):1068–1073.
2. Weiden PL, Sullivan KM, Flournoy N, Storb R, Thomas ED. Antileukemic effect of chronic graft-versus-host disease: contribution to improved survival after allogeneic marrow transplantation. *N Engl J Med.* 1981;304(25):1529–1533.
3. Korngold R, Sprent J. Lethal graft-versus-host disease after bone marrow transplantation across minor histocompatibility barriers in mice. Prevention by removing mature T-cells from marrow. *J Exp Med.* 1978;148(6):1687–1698.
4. Apperley JF, Jones L, Hale G, Goldman JM. Bone marrow transplantation for chronic myeloid leukemia: T-cell depletion with Campath-1 reduces the incidence of acute graft-versus-host disease but may increase the risk of leukemia relapse. *Bone Marrow Transplant.* 1986;1(1):53–66.
5. Atkinson K, et al. Risk factors for chronic graft-versus-host disease after HLA-identical sibling bone marrow transplantation. *Blood.* 1990;75(12):2459–2464.
6. Shlomchik WD, et al. Prevention of graft versus host disease by inactivation of host antigen-presenting cells. *Science.* 1999;285(5426):412–415.
7. Reddy P, Maeda Y, Liu C, Krijanovski OI, Korngold R, Ferrara JL. A crucial role for antigen-presenting cells and alloantigen expression in graft-versus-leukemia responses. *Nat Med.* 2005;11(11):1244–1249.
8. Bleakley M, Riddell SR. Molecules and mechanisms of the graft-versus-leukaemia effect. *Nat Rev Cancer.* 2004;4(5):371–380.
9. Teshima T, et al. Acute graft-versus-host disease does not require alloantigen expression on host epithelium. *Nat Med.* 2002;8(6):575–581.
10. Jones SC, Murphy GF, Friedman TM, Korngold R. Importance of minor histocompatibility antigen expression by nonhematopoietic tissues in a CD4+ T cell-mediated graft-versus-host disease model. *J Clin Invest.* 2003;112(12):1880–1886.
11. Ruggeri L, et al. Effectiveness of donor natural killer cell alloreactivity in mismatched hematopoietic transplants. *Science.* 2002;295(5562):2097–2100.
12. Matte CC, et al. Donor APCs are required for maximal GVHD but not for GVL. *Nat Med.* 2004;10(9):987–992.
13. Cooke KR, et al. An experimental model of idiopathic pneumonia syndrome after bone marrow transplantation. I. The roles of minor H antigens and endotoxin. *Blood.* 1996;88(8):3230–3239.
14. Korngold R, Sprent J. Features of T cells causing H-2-restricted lethal graft-vs.-host disease across minor histocompatibility barriers. *J Exp Med.* 1982;155(3):872–883.
15. Zhang Y, Joe G, Hexner E, Zhu J, Emerson SG. Alloreactive memory T cells are responsible for the persistence of graft-versus-host disease. *J Immunol.* 2005;174(5):3051–3058.
16. Stefanova I, Dorfman JR, Germain RN. Self-recognition promotes the foreign antigen sensitivity of naive T lymphocytes. *Nature.* 2002;420(6914):429–434.
17. Zhang Y, Louboutin JP, Zhu J, Rivera AJ, Emerson SG. Preterminal host dendritic cells in irradiated mice prime CD8+ T cell-mediated acute graft-versus-host disease. *J Clin Invest.* 2002;109(10):1335–1344.
18. Zajac AJ, et al. Viral immune evasion due to persistence of activated T cells without effector function. *J Exp Med.* 1998;188(12):2205–2213.
19. Barber DL, et al. Restoring function in exhausted CD8 T cells during chronic viral infection. *Nature.* 2006;439(7077):682–687.
20. Shin H, Wherry EJ. CD8 T cell dysfunction during chronic viral infection. *Curr Opin Immunol.* 2007;19(4):408–415.
21. Keir ME, Butte MJ, Freeman GJ, Sharpe AH. PD-1 and its ligands in tolerance and immunity. *Annu Rev Immunol.* 2008;26:677–704.
22. Dong H, et al. Tumor-associated B7-H1 promotes T-cell apoptosis: a potential mechanism of immune evasion. *Nat Med.* 2002;8(8):793–800.
23. Ahmadzadeh M, et al. Tumor antigen-specific CD8

T cells infiltrating the tumor express high levels of PD-1 and are functionally impaired. *Blood.* 2009; 114(8):1537–1544.
24. Zhang L, Gajewski TF, Kline J. PD-1/PD-L1 interactions inhibit anti-tumor immune responses in a murine acute myeloid leukemia model. *Blood.* 2009; 114(8):1545–1552.
25. Mumprecht S, Schurch C, Schwaller J, Solenthaler M, Ochsenbein AF. PD-1 signaling on chronic myeloid leukemia-specific T cells results in T cell exhaustion and disease progression. *Blood.* 2009; 114(8):1528–1536.
26. Iwai Y, Terawaki S, Ikegawa M, Okazaki T, Honjo T. PD-1 inhibits antiviral immunity at the effector phase in the liver. *J Exp Med.* 2003;198(1):39–50.
27. Horowitz MM, et al. Graft-versus-leukemia reactions after bone marrow transplantation. *Blood.* 1990;75(3):555–562.
28. Gallimore A, et al. Induction and exhaustion of lymphocytic choriomeningitis virus-specific cytotoxic T lymphocytes visualized using soluble tetrameric major histocompatibility complex class I-peptide complexes. *J Exp Med.* 1998;187(9):1383–1393.
29. Welsh RM. Assessing CD8 T cell number and dysfunction in the presence of antigen. *J Exp Med.* 2001; 193(5):F19–F22.
30. Moskophidis D, Lechner F, Pircher H, Zinkernagel RM. Virus persistence in acutely infected immunocompetent mice by exhaustion of antiviral cytotoxic effector T cells. *Nature.* 1993;362(6422):758–761.
31. Appay V, et al. HIV-specific CD8(+) T cells produce antiviral cytokines but are impaired in cytolytic function. *J Exp Med.* 2000;192(1):63–75.
32. Xiong Y, et al. Simian immunodeficiency virus (SIV) infection of a rhesus macaque induces SIV-specific CD8(+) T cells with a defect in effector function that is reversible on extended interleukin-2 incubation. *J Virol.* 2001;75(6):3028–3033.
33. Pantaleo G, Harari A. Functional signatures in antiviral T-cell immunity for monitoring virus-associated diseases. *Nat Rev Immunol.* 2006;6(5):417–423.
34. Tham EL, Mescher MF. Signaling alterations in activation-induced nonresponsive CD8 T cells. *J Immunol.* 2001;167(4):2040–2048.
35. Tham EL, Shrikant P, Mescher MF. Activation-induced nonresponsiveness: a Th-dependent regulatory checkpoint in the CTL response. *J Immunol.* 2002;168(3):1190–1197.
36. Boissonnas A, et al. Antigen distribution drives programmed antitumor CD8 cell migration and determines its efficiency. *J Immunol.* 2004;173(1):222–229.
37. Saito T, Dworacki G, Gooding W, Lotze MT, Whiteside TL. Spontaneous apoptosis of CD8+ T lymphocytes in peripheral blood of patients with advanced melanoma. *Clin Cancer Res.* 2000;6(4):1351–1364.
38. Fontaine P, Roy-Proulx G, Knafo L, Baron C, Roy DC, Perreault C. Adoptive transfer of minor histocompatibility antigen-specific T lymphocytes eradicates leukemia cells without causing graft-versus-host disease. *Nat Med.* 2001;7(7):789–794.
39. Meunier MC, Roy-Proulx G, Labrecque N, Perreault C. Tissue distribution of target antigen has a decisive influence on the outcome of adoptive cancer immunotherapy. *Blood.* 2003;101(2):766–770.
40. Dickinson AM, et al. In situ dissection of the graft-versus-host activities of cytotoxic T cells specific for minor histocompatibility antigens. *Nat Med.* 2002; 8(4):410–414.
41. Ding ZC, Blazar BR, Mellor AL, Munn DH, Zhou G. Chemotherapy rescues tumor-driven aberrant CD4+ T-cell differentiation and restores an activated polyfunctional helper phenotype. *Blood.* 2010; 115(12):2397–2406.
42. Tanaka K, et al. PDL1 is required for peripheral transplantation tolerance and protection from chronic allograft rejection. *J Immunol.* 2007; 179(8):5204–5210.
43. Haspot F, et al. Peripheral deletional tolerance of alloreactive CD8 but not CD4 T cells is dependent on the PD-1/PD-L1 pathway. *Blood.* 2008; 112(5):2149–2155.
44. Yamazaki T, et al. Expression of programmed death 1 ligands by murine T cells and APC. *J Immunol.* 2002;169(10):5538–5545.
45. Keir ME, et al. Tissue expression of PD-L1 mediates peripheral T cell tolerance. *J Exp Med.* 2006; 203(4):883–895.
46. Crawford A, Wherry EJ. The diversity of costimulatory and inhibitory receptor pathways and the regulation of antiviral T cell responses. *Curr Opin Immunol.* 2009;21(2):179–186.
47. Blackburn SD, et al. Coregulation of CD8+ T cell exhaustion by multiple inhibitory receptors during chronic viral infection. *Nat Immunol.* 2009; 10(1):29–37.
48. Petrovas C, et al. PD-1 is a regulator of virus-specific CD8+ T cell survival in HIV infection. *J Exp Med.* 2006;203(10):2281–2292.
49. Brooks DG, Trifilo MJ, Edelmann KH, Teyton L, McGavern DB, Oldstone MB. Interleukin-10 determines viral clearance or persistence in vivo. *Nat Med.* 2006;12(11):1301–1309.
50. Blackburn SD, Shin H, Freeman GJ, Wherry EJ. Selective expansion of a subset of exhausted CD8 T cells by alphaPD-L1 blockade. *Proc Natl Acad Sci U S A.* 2008;105(39):15016–15021.
51. Kaufmann DE, et al. Upregulation of CTLA-4 by HIV-specific CD4+ T cells correlates with disease progression and defines a reversible immune dysfunction. *Nat Immunol.* 2007;8(11):1246–1254.
52. Franceschini D, et al. PD-L1 negatively regulates CD4+CD25+Foxp3+ Tregs by limiting STAT-5 phosphorylation in patients chronically infected with HCV. *J Clin Invest.* 2009;119(3):551–564.
53. Socie G, Blazar BR. Acute graft-versus-host disease: from the bench to the bedside. *Blood.* 2009; 114(20):4327–4336.
54. Blazar BR, et al. Blockade of programmed death-1 engagement accelerates graft-versus-host disease lethality by an IFN-gamma-dependent mechanism. *J Immunol.* 2003;171(3):1272–1277.
55. Brochu S, Rioux-Masse B, Roy J, Roy DC, Perreault C. Massive activation-induced cell death of alloreactive T cells with apoptosis of bystander postthymic T cells prevents immune reconstitution in mice with graft-versus-host disease. *Blood.* 1999;94(2):390–400.
56. Dey B, et al. The fate of donor T-cell receptor transgenic T cells with known host antigen specificity in a graft-versus-host disease model. *Transplantation.* 1999;68(1):141–149.
57. Choi EY, et al. Real-time T-cell profiling identifies H60 as a major minor histocompatibility antigen in murine graft-versus-host disease. *Blood.* 2002; 100(13):4259–4265.
58. Michalek J, Collins RH, Hill BJ, Brenchley JM, Douek DC. Identification and monitoring of graft-versus-host specific T-cell clone in stem cell transplantation. *Lancet.* 2003;361(9364):1183–1185.
59. Hirano F, et al. Blockade of B7-H1 and PD-1 by monoclonal antibodies potentiates cancer therapeutic immunity. *Cancer Res.* 2005;65(3):1089–1096.
60. Ando K, et al. Perforin, Fas/Fas ligand, and TNF-alpha pathways as specific and bystander killing mechanisms of hepatitis C virus-specific human CTL. *J Immunol.* 1997;158(11):5283–5291.
61. Tsushima F, et al. Preferential contribution of B7-H1 to programmed death-1-mediated regulation of hapten-specific allergic inflammatory responses. *Eur J Immunol.* 2003;33(10):2773–2782.
62. Teshima T, et al. IL-11 separates graft-versus-leukemia effects from graft-versus-host disease after bone marrow transplantation. *J Clin Invest.* 1999;104(3):317–325.

Published January 31, 2011

JEM

Article

The Wnt agonist R-spondin1 regulates systemic graft-versus-host disease by protecting intestinal stem cells

Shuichiro Takashima,[1] Masanori Kadowaki,[1] Kazutoshi Aoyama,[1] Motoko Koyama,[1] Takeshi Oshima,[3] Kazuma Tomizuka,[3] Koichi Akashi,[1,2] and Takanori Teshima[2]

[1]Department of Medicine and Biosystemic Science and [2]Center for Cellular and Molecular Medicine, Kyushu University Graduate School of Medical Science, Higashi-ku, Fukuoka 812-8582, Japan
[3]Innovative Drug Research Laboratories, Kyowa Hakko Kirin Co., Ltd., Machida, Tokyo 194-8533, Japan

Graft-versus-host disease (GVHD) is a major complication of allogeneic bone marrow transplantation (BMT), and damage to the gastrointestinal (GI) tract plays a critical role in amplifying systemic disease. Intestinal stem cells (ISCs) play a pivotal role not only in physiological tissue renewal but also in regeneration of the intestinal epithelium after injury. In this study, we have discovered that pretransplant conditioning regimen damaged ISCs; however, the ISCs rapidly recovered and restored the normal architecture of the intestine. ISCs are targets of GVHD, and this process of ISC recovery was markedly inhibited with the development of GVHD. Injection of Wnt agonist R-spondin1 (R-Spo1) protected against ISC damage, enhanced restoration of injured intestinal epithelium, and inhibited subsequent inflammatory cytokine cascades. R-Spo1 ameliorated systemic GVHD after allogeneic BMT by a mechanism dependent on repair of conditioning-induced GI tract injury. Our results demonstrate for the first time that ISC damage plays a central role in amplifying systemic GVHD; therefore, we propose ISC protection by R-Spo1 as a novel strategy to improve the outcome of allogeneic BMT.

CORRESPONDENCE
Takanori Teshima:
tteshima@
cancer.med.kyushu-u.ac.jp

Abbreviations used: BMT, BM transplantation; GI, gastrointestinal; GVHD, graft-versus-host disease; ISC, intestinal stem cell; R-Spo1, R-spondin1; SCT, stem cell transplantation; TBI, total body irradiation; TCD, T cell depleted.

An important aspect of cancer therapy is maintaining a fine balance between the use of chemoradiotherapy doses high enough to kill tumor cells and doses low enough to prevent damage to normal tissue. The gastrointestinal (GI) epithelium and BM are the most rapidly self-renewing tissues in adults and are therefore susceptible to cytotoxic exposure, showing a rapid expression of damage. Damage to these tissues is a dose-limiting and potentially lethal toxicity of chemoradiotherapy used to treat cancer patients. Allogeneic hematopoietic stem cell transplantation (SCT) is a curative therapy for hematologic malignancies that works by delivering healthy hematopoietic stem cells to replace BM destroyed by the high-dose chemoradiotherapy (pretransplant conditioning); however, this process is complicated by regimen-related toxicity against other tissues, particularly in the GI tract.

Graft-versus-host disease (GVHD), a major and devastating complication of allogeneic SCT, is a complex process involving donor T cell responses to host antigens and the dysregulation of inflammatory cytokine cascades (Hill et al., 1997; Hill and Ferrara, 2000; Teshima et al., 2002a; Ferrara et al., 2003). Increasing evidence from experimental and clinical SCT suggests that conditioning-mediated GI tract damage plays a central role in amplifying GVHD by propagating its cytokine storm characteristics (Hill et al., 1997; Hill and Ferrara, 2000; Ferrara et al., 2003). Intestinal epithelial cells are continuously regenerated from intestinal stem cells (ISCs), which are key to the regeneration of damaged intestinal epithelium (Batlle et al., 2002; Pinto et al., 2003; Barker et al., 2007, 2008). However, the dynamic process of damage and repopulation of ISCs, which play a pivotal

The Rockefeller University Press $30.00
J. Exp. Med. Vol. 208 No. 2 285-294
www.jem.org/cgi/doi/10.1084/jem.20101559

Supplemental Material can be found at:
http://jem.rupress.org/content/suppl/2011/01/31/jem.20101559.DC1.html

Published January 31, 2011

role in the competitive race between tissue damage and restoration during conditioning regimens and GVHD, is not well understood.

Wnt signaling plays a critical role in the regulation of intestinal epithelial cell proliferation during their maturation or regeneration (Batlle et al., 2002; Pinto et al., 2003; Reya and Clevers, 2005; Barker et al., 2008). R-spondin1 (R-Spo1) is a potent activator of the Wnt signaling pathway. It relieves the Dickkopf-1 inhibition imposed on the Wnt signaling pathway and thereby increases levels of the Wnt pathway coreceptor low-density lipoprotein receptor–related protein-6 on cell surface (Kim et al., 2005; Binnerts et al., 2007). We have previously shown that human R-Spo1 transgenic mice had a marked thickening of the mucosa and displayed crypt epithelial hyperplasia (Kim et al., 2005). Injection of human R-Spo1 induced rapid onset of crypt cell proliferation in the intestine of normal mice through β-catenin stabilization and subsequent transcriptional activation of target genes (Kim et al., 2005). Thus, injection of R-Spo1 protected mice from chemotherapy- or radiation-induced colitis by stimulating mucosal regeneration and restoring intestinal architecture (Kim et al., 2005; Zhao et al., 2007, 2009; Bhanja et al., 2009). However, because of the lack of specific markers for ISCs, it is unclear whether this result was mediated by the direct effect of R-Spo1 on ISCs.

In this study, we investigated the dynamic process of ISC damage and repopulation during the pretransplant conditioning regimen, total body irradiation (TBI), and GVHD. The effects of R-Spo1 on this process were also examined using recently identified markers for ISCs such as *Lgr5* (*leucine-rich repeat–containing G protein–coupled receptor 5*) and *Olfm4* (*Olfactomedin-4*; Barker et al., 2007, 2008; van der Flier et al., 2009a,b). *Lgr5* and *Olfm4* mark rapidly cycling crypt base columnar cells, which can give rise to all intestinal epithelial lineages (Barker et al., 2007, 2008; van der Flier et al., 2009a,b). We then tested the hypothesis that protection of ISCs improves the outcome of allogeneic SCT by regulating systemic GVHD using a well-characterized murine model of MHC-mismatched, haploidentical BM transplantation (BMT).

RESULTS

R-Spo1 protected against radiation-induced colitis by stimulating proliferation of ISCs through the Wnt signaling pathway

We first studied the effect of R-Spo1 on the expression of Wnt target genes in the small intestine using quantitative real-time PCR. Injection of R-Spo1 (200 μg/day) over 3 d significantly up-regulated the expression of Wnt target genes, including *Axin2*, *Ascl2* (*Achaete scute-like 2*), and *Lgr5* (Fig. S1 A). We noted an elongation of villi with an increased number of *Olfm4*$^+$ ISCs in the crypts of R-Spo1–treated animals (Fig. S1, B and C). Ki-67 immunostaining also showed crypt hyperplasia paralleling an increased number of Ki-67$^+$ cycling cells in the crypts (Fig. S1, D and E).

Next, we evaluated the effect of R-Spo1 administration on the process of mucosal regeneration after TBI. According to our preliminary experiments (unpublished data), mice irradiated with 15 Gy TBI on day 0 were intravenously injected with 200 μg R-Spo1 once daily from day −3 to −1 and from day 1–3. The real-time PCR analysis of the small intestine harvested 6 h after the final administration of R-Spo1 showed up-regulated expression of *Axin2* and *Ascl2* in R-Spo1–treated mice (Fig. 1 A). The *Olfm4*$^+$ cell population was significantly greater in R-Spo1–treated mice than in controls on day 3 (Fig. 1, B and C); as a result, radiation colitis characterized

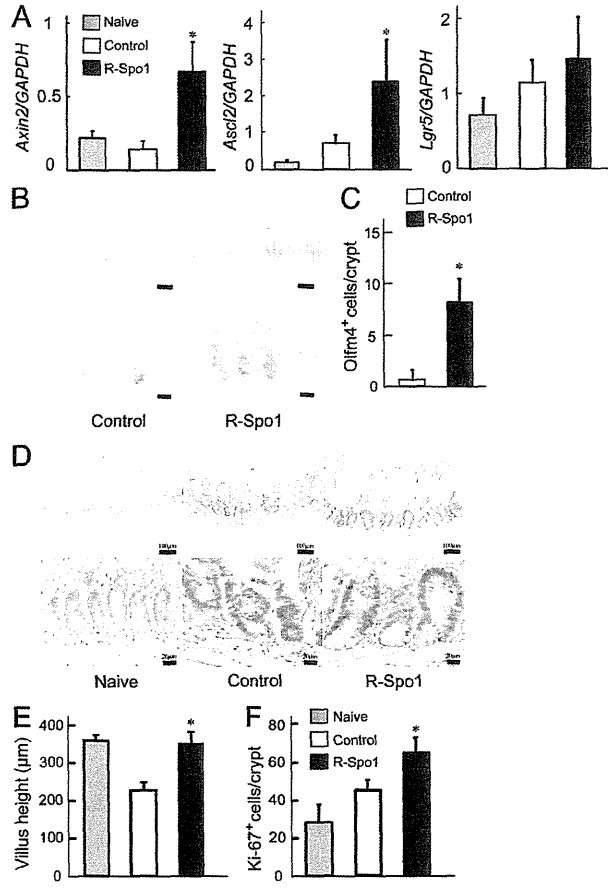

Figure 1. R-Spo1 protected against radiation-induced colitis by enhancing proliferation of ISCs via the Wnt signaling pathway. B6D2F1 mice irradiated with 15 Gy TBI on day 0 and intravenously injected with R-Spo1 (200 μg/day) or control from day −3 to −1 and day 1–3. The small intestine was harvested 6 h after the final administration of R-Spo1 for quantitative real-time PCR analysis and in situ hybridization, and 24 h later for immunohistochemistry. (A) Quantitative real-time PCR analysis of *Axin2*, *Ascl2*, and *Lgr5* transcripts normalized to those of GAPDH (naive, $n = 3$; control, $n = 4$; R-Spo1, $n = 4$). (B) In situ hybridization for *Olfm4* on representative crypts. (C) Quantification of *Olfm4*$^+$ cells per crypt ($n = 4$ per group). (D) Ki-67 staining of the terminal ileum. (E) Villus height of the terminal ileum (naive, $n = 3$; control, $n = 4$; R-Spo1, $n = 4$). (F) Quantification of Ki-67$^+$ cells per crypt (naive, $n = 3$; control, $n = 4$; R-Spo1, $n = 4$). Data are representative of two independent experiments and are shown as means ± SD. *, $P < 0.05$ compared with control. Bars: (B and D, top row) 100 μm; (B and D, bottom row) 20 μm.

Published January 31, 2011

by blunting of villi was significantly reduced in R-Spo1–treated animals (Fig. 1, D and E). We also noted crypt hyperplasia and an increased number of Ki-67$^+$ cycling cells in the crypt on day 4 (Fig. 1, D and F). These results extend our previous observations regarding R-Spo1–mediated mitogenic effects on the intestinal epithelium (Kim et al., 2005) by documenting the effects of R-Spo1 on ISCs.

R-Spo1 protected against ISC damage after allogeneic BMT

GI tract damage is much more severe in allogeneic SCT than in autologous or syngeneic SCT because of the additional detrimental effects of GVHD on the GI tract. However, it remains to be elucidated whether GVHD targets ISCs that are crucial for the regeneration of damaged intestinal epithelium and also how the damage and repopulation of ISCs affects the process of mucosal injury and regeneration after allogeneic BMT. To address these issues, lethally irradiated B6D2F1 mice were transplanted with 5 × 10^6 T cell–depleted (TCD) BM cells with or without 2 × 10^6 T cells from MHC-mismatched C57BL/6 (B6) or B6-Ly5.1 donors on day 0. Small intestines were harvested from mice on day 0 before TBI and on days 3 and 6 after BMT, and quantitative real-time PCR and in situ hybridization were performed to determine the kinetics of loss and repopulation of *Olfm4*$^+$ ISCs. R-Spo1 was injected from day −3 to −1 and day 1–3 after BMT. TCD animals and control-treated allogeneic animals served as non-GVHD

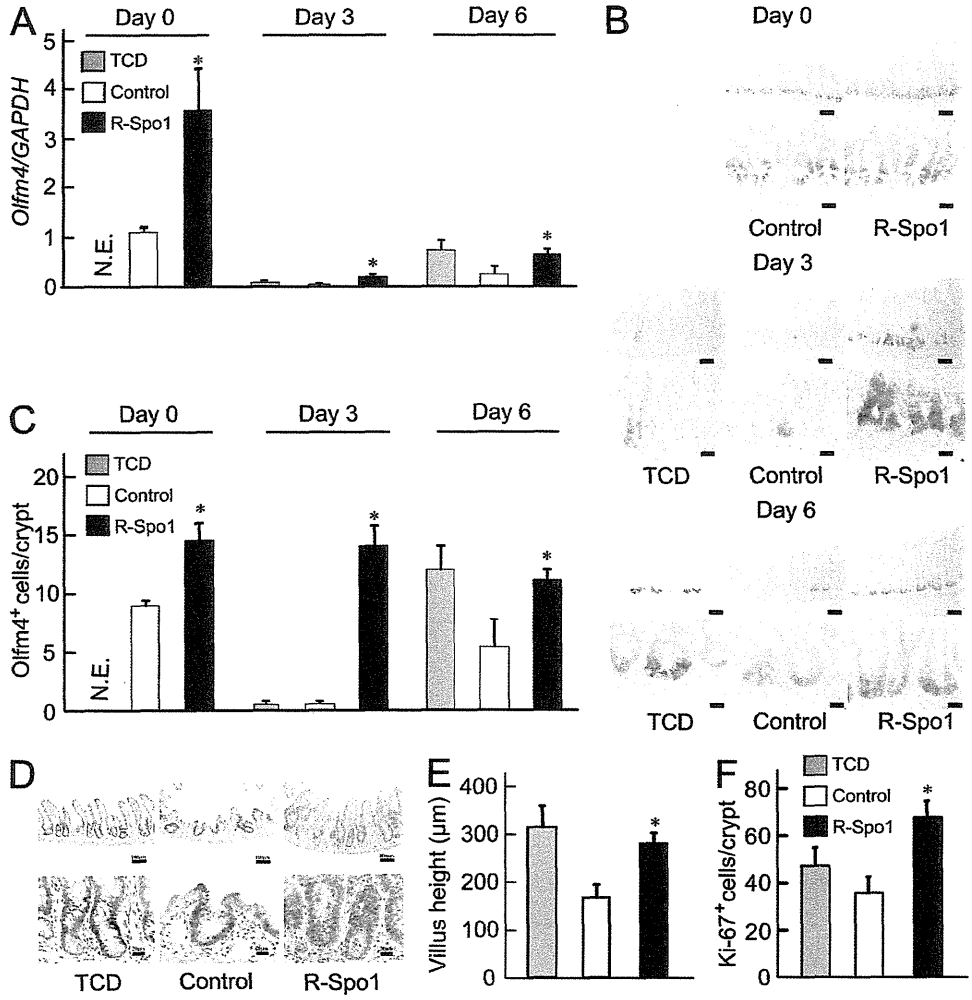

Figure 2. R-Spo1 enhanced repopulation of ISCs after allogeneic BMT. Lethally irradiated B6D2F1 mice were transplanted with 5 × 10^6 TCD BM with or without 2 × 10^6 T cells from B6 donors on day 0. R-Spo1 (200 μg/day) or control was intravenously injected from day −3 to −1 and day 1–3 after BMT. Small intestines were harvested on day 0 (before TBI) and days 3 and 6. (A) Quantitative real-time PCR analysis of *Olfm4* transcripts normalized to those of GAPDH (TCD, $n = 3$; control, $n = 4$; R-Spo1, $n = 4$ per time point). (B) In situ hybridization of *Olfm4* on representative crypts. (C) Quantification of *Olfm4*$^+$ cells per crypt (TCD, $n = 3$; control, $n = 4$; R-Spo1, $n = 4$ per time point). (D) Ki-67 staining of the terminal ileum harvested on day 6. (E) Villus height of the terminal ileum was measured as described in Fig. 1 E using the slides in D (TCD, $n = 3$; control, $n = 5$; R-Spo1, $n = 5$). (F) Quantification of Ki-67$^+$ cells per crypt (TCD, $n = 3$; control, $n = 5$; R-Spo1, $n = 5$). Data are representative of two independent experiments and are shown as means ± SD. *, $P < 0.05$ compared with control. Bars: (B and D, top rows) 100 μm; (B and D, bottom rows) 20 μm.